SIMULATION OF BIOMASS GASIFICATION IN BUBBLING FLUIDIZED BED REACTOR USING ASPEN PLUS®

M. Puig-Gamero[1], D.T. Pio[2], LA.C. Tarelho[2], P. Sánchez[1], L. Sanchez- Silva[1*]

[1]Department of Chemical Engineering, University of Castilla –La Mancha, Avda. Camilo José Cela 12, 13071 Ciudad Real, Spain

[2]Department of Environment and Planning and Centre of Environmental and Marine Studies, University of Aveiro, Campus Universitário de Santiago, 3810-193 Aveiro, Portugal

*Corresponding author phone: +34 926 29 53 00 ext. 6307

e-mail: marialuz.sanchez@uclm.es

Nomenclature

CFD	Computational Fluid Dynamics	$Y_{ch,F}$	Char yield of pyrolysis process
LHV	Lower Heating Value	$Y_{H2,F}$	H_2 yield of pyrolysis process
CGE	Cold Gas Efficiency	$Y_{CO,F}$	CO yield of pyrolysis process
BFB	Bubbling Fluidized Bed	$Y_{H2O,F}$	H_2O yield of pyrolysis process
RFB	Residual Forest Biomass	$Y_{CO2,F}$	CO_2 yield of pyrolysis process
db	Dry basis	$Y_{C, bio}$	Carbon content of biomass
wb	Wet basis	$Y_{H, bio}$	Hydrogen content of biomass
VM	Volatile Matter	$Y_{O, bio}$	Oxygen content of biomass
FC	Fixed Carbon	$Y_{C, char}$	Carbon content of char
nd	Non-determined	$Y_{H, char}$	Hydrogen content of char
ER	Equivalence Ratio	$Y_{O, char}$	Oxygen content of char
NPT	Normal pressure (1.013×10^5 Pa) and temperature (273 K)	$Y_{C, tar}$	Carbon content of tar
IGT	Institute of Gas Technology	$Y_{H, tar}$	Hydrogen content of tar
		$Y_{O, tar}$	Oxygen content of tar
		V_G	Volumetric gas flow rate of the dry gas produced (Nm^3/s)
		PG	Absolute pressure (Pa)
		TG	Absolute temperature (K)
		R	Ideal gas constant (J/molK)
		$\varepsilon_{c,CO2}$	Molar fraction of carbon in CO_2
		$\varepsilon_{c,CO}$	Molar fraction of carbon in CO
		$y_{,i}$	Molar fraction of CO_2, CO CH_4, and C_2H_4 in the dry gas produced
		m_F	Biomass mass flow rate (kg_{db}/s)
		W_{FC}	Mass fraction of carbon in the biomass (kg C/kg biomass $_{db}$)

14

Abstract

The direct (with air) gasification process of biomass in bubbling fluidized bed reactor was simulated using Aspen Plus®. The reactor was divided in three parts: the pyrolysis zone, combustion zone and reduction zone. The pyrolysis process simulation was supported by an external MS-Excel® subroutine to define the yield and composition of the main components, namely, char, gas and tar. Whereas the combustion and reduction processes were simulated using a kinetic model. These models were calibrated and thereafter validated with a set of distinct results from gasification of four different types of biomass using a pilot-scale bubbling fluidized bed reactor, with different equivalence ratio (from 0.17 to 0.35) and temperature (from 709 ºC to 859 ºC). The results obtained from the simulation, namely the concentration of CO, CO_2, H_2, CH_4, C_2H_4 in the producer gas, were in good agreement with the experimental ones for a set of biomass types and operating conditions. Amongst the gases analysed, H_2 gas was predicted with the lowest accuracy, always being overestimated; despite that, the highest absolute error obtained for H_2 was only 4.4%. Finally, the tar concentration predicted was between 20 and 42 g/Nm^3 and it decreased with the increase of equivalence ratio, temperature and biomass particle size.

Keywords: biomass, gasification, bubbling fluidized bed, kinetic modelling, Aspen Plus®

1. Introduction

In recent years, the gasification process has taken great interest because the gas producer gas can be used in several applications, depending on its characteristics. The producer gas can be burnt directly, e.g., fuel in furnaces or boilers or in gas turbine, or used to produce added value chemicals [1]. However, the gasification process is complex, and it is difficult to predict accurately the producer gas composition. Although the main gases are H_2O, CO_2, CO, CH_4, C_2H_4 and H_2, the amount of these gases and tar are unknown and can vary in a wide range depending on biomass characteristics, type of reactor, gasifying agent and operating conditions [2]. Regarding tar, it is a complex blend of high molecular weight hydrocarbons formed during the gasification process, which condense in the form of a viscous liquid in the gasifier pipe outlets and filters, consequently leading to blockages and clogging, and causing downstream problems [3, 4]. In addition to the operating problems in the gasifier and downstream equipment, a high tar content in the gas product makes it unsuitable for many commercial applications. In this sense, tar should be as low as possible and always below than 1 g/Nm^3, albeit this value depending on the final application [5]. Accordingly, predicting the gas composition is a difficult task. For example, chemical equilibrium has been often referred as a tool to predict producer gas composition from biomass gasification, but recent analysis on the subject [6] shows that this approach does not offers accurate predictions of producer gas composition during biomass gasification in bubbling fluidised reactor; for example, significant overestimation of H_2 and CO concentration and underestimation of CH_4 concentration is observed.

Hence, process simulation is an increasingly important and effective tool to support the development and implementation of the gasification process, being a quantitative tool for understanding and optimizing the process [1]. In addition, it is very useful for its analysis,

65 evaluation and design [7]. Moreover, it can reduce the high costs related to extensive
66 experimental demonstration and allow to study different scenarios saving time and costs
67 [5]. For modelling biomass gasification in fluidized bed reactors two main approaches
68 have been commonly used: (i) process simulation using computational fluid dynamics
69 (CFD) tools as Barracuda, MFIX, or OpenFOAM, ANSYS and (ii) process simulation
70 using Aspen Plus. In this sense, a significant number of authors [8-14] has been often
71 using CFD to simulate the gasification process, namely with focus on mass and heat
72 transfer and fluid dynamic effects within the reactive system. This type of modelling
73 approach requires comprehensive design involving geometry, meshing, simulation set-up
74 and is time consuming in respect of convergence, requiring high computational
75 resources[15]. Moreover, the existing numerical methods can be generally categorized as
76 Eulerian-based methods (two-fluid model) and Lagrangian-based methods (discrete
77 element method and multiphase particle in cell) [16]. The CFD simulations are limited
78 by the calculation of the physical properties of the compounds. Since an accurate
79 modelling of the physical properties of compounds requires developing and implementing
80 in the CFD simulator complex user defined subroutines. Thus, the main challenge
81 associated to chemical engineering CFD simulations is to obtain an accurate modelling
82 of the physical properties in conditions either of ideality or of non-ideality behaviour from
83 any set of pressure, temperature and composition [17]. On the other hand, modelling
84 biomass gasification on Aspen Plus® has been gained relevance [3] due to extensive
85 database of compounds and thermodynamic models available in the toolbox. In addition,
86 its suitability to handle solid materials (e.g., biomass), which results from its wide
87 properties database, including physical properties data [17]. Other advantages of this
88 software are the high flexibility regarding different process configurations, which allows
89 to optimize varying operational conditions and to determine limitations of processes

subject to these conditions. Moreover, if suitable thermodynamic data, realistic operating conditions and precise equipment models are adopted, the real behaviour of the process is argued to be predicted with accuracy [3]. In addition, Aspen Plus software allows the integration of upstream and downstream processes, such as biomass drying and crushing, gas cleaning and combustion systems or chemical synthesis. Therefore, Aspen Plus simulator can be considered as a useful tool to plan new processes and develop existing ones [3].

According to Beheshti et al. (2015) [18], there are two different approaches to model gasification process using Aspen Plus® simulator: thermodynamic equilibrium modelling or kinetic modelling. The thermodynamic equilibrium models can be stoichiometric or non-stoichiometric and are based on the Gibbs free energy. They can be implemented based on defining a set of reactions and then calculating the equilibrium composition (stoichiometric approach), or by defining the set of chemical elements in the feeding and compounds in the output and calculate the composition that minimizes the Gibbs free energy of the system (non-stoichiometric approach). Its use involves different hypothesis: the gasifier is dimensionless and there is a perfect mixture in it, so the temperature is uniform, the reaction rates are fast enough, and the residence time is also long enough to reach the chemical equilibrium. However thermodynamic equilibrium does not seems suitable for predicting gasification gas composition in bubbling fluidized bed reactors [6] due to argued overestimation of H_2 and CO concentration and underestimation of CH_4 concentration [6]. On the other hand, the kinetic modeling approach is more complex to implement since this approach needs a detailed knowledge of the gasification reactions and respective kinetics, as also the reactor configuration, but the results are argued to be closer to experimental data [18].

There are some studies that simulate biomass gasification in fluidized bed reactors using Aspen Plus simulator. Marcantonio et al. [19] simulated H_2 production from biomass gasification in fluidized bed reactor with different separation systems using Aspen Plus. The authors concluded that the quasi-equilibrium model used give reasonable predictions for the gasification process. On the other hand, Lopes-Motta et al. [20] used Aspen Plus to simulated several scenarios of biomass gasification in distinct fluidized bed configurations, including the study of the influence of operating conditions and gasifying agent (steam and oxygen) on syngas composition and process performance. The authors determined that the temperature was crucial for higher H_2 and CO production, CO_2 consumption, higher syngas lower heating value (LHV) and higher cold gas efficiency (CGE) [20] . Kaushal et al. [21] studied the simulation of biomass gasification in a fluidized bed reactor using Aspen Plus considering the tar formation and its cracking kinetics in the model. The results showed that accounting for tar and its kinetics significantly improved the model performance in predicting the gas composition with accuracy [21].

However, there are a few studies that analyse and discuss essential modelling steps important to develop a robust tool to the simulation of direct (air) gasification process in bubbling fluidized bed (BFB) using Aspen Plus®. Thus, the innovative aspects of this work include the integration of i) implementation and evaluation of a kinetic mechanism in a model to simulate the process of biomass gasification and to predict the composition of the producer gas, ii) inclusion of tar formation predictions by means of an empirical model implemented in a subroutine, iii) model calibration and validation with experimental results from biomass gasification in a pilot-scale BFB reactor, iv) flexibility of the model to evaluate distinct fuel types, and iv) evaluation of effect of different kinetic

mechanisms and kinetic parameters to predict producer gas composition and efficiency parameters of the gasification process."

2. Materials and methods

2.1 Biomass characteristics

The biomass types selected include pine pellets (6 mm diameter and 15-20 mm in length) and chips from different types of residual forest biomass (RFB) derived from pine (particle size below 10mm) and eucalyptus (particle size below 5mm). Table 1 shows the proximate and elemental analysis of the biomass types selected.

Table 1. Proximate and elemental analysis of the biomass.

	Ultimate Analysis (wt.%, db)					***Proximate Analysis (wt.%, wb)***			
Biomass	***C***	***H***	***N***	***S***	***O^{diff}***	***Ash***	***VM***	***FC^{diff}***	***Moisture***
Pine pellet	47.50	6.20	0.09	nd	46.21	0.30	78.50	16.60	4.60
Eucalyptus type A	45.85	6.13	0.35	nd	47.67	2.87	71.00	14.60	11.80
Eucalyptus type B	49.07	6.45	0.07	nd	44.41	1.19	68.50	19.00	11.40
Pine RFB	50.80	6.50	0.25	nd	42.45	1.20	71.10	16.80	11.00

db, dry basis; wb: wet basis; O^{diff}: wt.% of oxygen calculated from difference of C, H, N and S; VM: Volatile matter; FC^{diff}: wt.% of fixed carbon calculated from difference from moisture, ash and volatile matter; nd – not determined, below the detection limit of the method (100 ppm wt).

2.2 Experimental facility

In this work, an autothermal pilot-scale BFB (80 kW_{th}) located at the Department of Environment and Planning at the University of Aveiro (Portugal) was used to get results to calibrate and then to validate the model. The experimental facility is described in detail in [2, 22, 23]. The reactor has an internal diameter of 0.25 m and height of 2.3 m. The bottom bed was composed by 17 kg of sand and the static bed height was of 0.23 m. The

157 gasification agent used was dry atmospheric air, which was fed through the distributor
158 plate. The BFB was operated at atmospheric pressure with a superficial gas velocity of
159 0.27 to 0.30 m/s (depending on the bed temperature in range 750 ºC to 860 ºC), which is
160 two times higher than the determined minimum fluidization velocity (0.14 m/s, bottom
161 bed particles with average granulometry of 700 μm). The biomass was fed above the
162 expanded bed surface, and at 0.3 m above the distributor plate, through a screw feeder.

163 Table 2 lists the operating conditions during the gasification experiments in the pilot
164 scale reactor. The bed temperature was maintained between 700 and 860 ºC and the
165 equivalence ratio (ER) between 0.17 and 0.35. The ER was calculated as the ratio between
166 the O_2 supplied to the gasifier and the stoichiometric O_2 for each biomass and it was
167 controlled by adjusting the biomass feeding rate while the primary air gas flow rate (200
168 L_{NPT}/min (NPT means normal pressure (1.013×10^5 Pa) and temperature (273K))
169 remained constant. Then, the direct gasifier operated under autothermal and steady state
170 conditions without any external auxiliary heating system, with required heat for the
171 gasification reactions being supported by the partial combustion of the biomass in the
172 reactor.

173 **Table 2.** Operating conditions during the gasification experiments in the pilot-scale [2].

Biomass	***Average bed Temperature (ºC)***	***Biomass feed rate (kg_{db}/h)***	***Equivalence ratio (ER)***
Pine pellet	816 ±17	12.5	0.22
	802 ±4	11.7	0.24
	854 ±6	10.9	0.25
	833 ±2	9.6	0.30
Eucalyptus type A	804 ±7	12.6	0.22
	798 ±8	11.6	0.24
	812 ±5	11.0	0.25
	810 ±9	10.6	0.26
	818 ±3	9.9	0.28
Eucalyptus type B	736 ±19	15.3	0.17

	709 ±14	14.4	0.18
	719 ±21	12.8	0.20
	800 ±5	10.0	0.25
	813 ±14	7.3	0.35
	786 ±12	10.8	0.23
Pine RFB	811 ±3	10.1	0.26
	830 ±2	8.9	0.30

db – means dry basis

2.3 Aspen plus modelling

Aspen Plus® simulation software was used to simulate the autothermal pilot-scale BFB. A sequential modular simulation approach has been developed to simulate a fluidized bed reactor. For this, the reactor was divided into several blocks to facilitate model convergence. As shown in Figure 1, the simulation was made considering the process divided in three successive sub-processes pyrolysis process (R-1), that also includes the drying step, oxidation process (R-3) and reduction process (R-4), as shown in the scheme of Figure 2 and Table 3. Moreover, Table 4 shows the chemical reactions and respective kinetic expressions considered in R-3 and R-4 blocks.

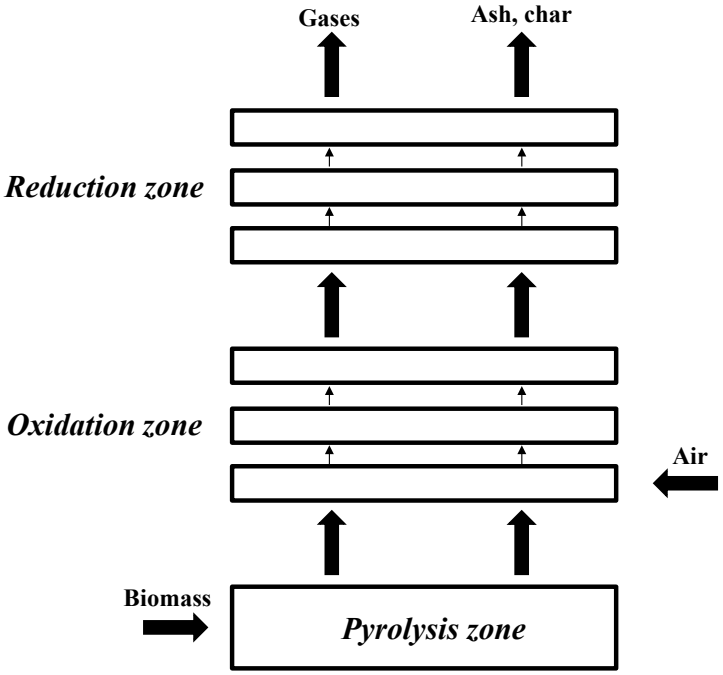

Figure 1. Overview of the gasifier model.

In the simulation, the biomass and char were defined as non-conventional components, and its proximate and elemental analysis was specified in ULTANAL and PROXANAL models. HCOALGEN and DCOALIGT models were used to obtain enthalpy and density, respectively, of non-conventional components as biomass and char. HCOALGEN includes different correlations for the calculation of heat capacity, heat of combustion and heat of formation. The heat of formation is calculated based on the heat of combustion of the biomass and the heat of formation of the products. To calculate the heat of combustion, the HCOALGEN uses proximate and elemental composition of the biomass and different types of correlations which are available in the Aspen Plus® [24]. The DCOALIGHT model is based on IGT (Institute of Gas Technology) correlation and ULTANAL is required. The ash was selected as non-conventional component and 100% of ash was established for the ultimate and proximate analysis. The fluid-dynamic package selected was Peng-Robinson with Boston Mathias function, due to being the most suitable for high temperature gasification processes, argued by [25]. The compounds

H_2, O_2, CO, CO_2, CH_4, C_2H_4, H_2O, N_2, NH_3, C_6H_6, C_6H_6O and $C_{10}H_8$ were defined as fluids and elemental C and S as solid phase.

The main assumptions considered in this simulation were the following

1. Ash was inert;
2. Process was in steady-state;
3. Pressure was uniform inside the reactor;
4. No heat and pressure losses took place in the reactor;
5. All gaseous compounds have ideal gas behaviour;
6. NH_3 and H_2S were not considered;
7. Unconverted solid carbon was present in the products;
8. Tar composition was assumed to be C_6H_6, C_6H_6O and $C_{10}H_8$;
9. This approach was 1D;
10. The fluidization velocity in the reactor was not considered as parameter in the model;
11. Arrhenius kinetics were considering for each reaction.

Figure 2 shows the Aspen Plus® flowsheet for the biomass gasification process and Table 3 lists a brief explanation of the blocks used. The biomass (Stream 1) was fed under ambient conditions (25 ºC and 1 atm) to the block R-1 to simulate an instant drying and pyrolysis process. In the Aspen Plus® modelling approach it is considered that the fuel drying and devolatilization processes are considered as occurring as two independent one step processes, time independent, just to deliver the water and the pyrolysis products as inputs to the subsequent gasification model. The biomass drying and pyrolysis process was simulated using an existing model [26], that delivered data on products char, gas and tar; this data was delivered to an external Excel subroutine that further supported

information to the model in Aspen Plus®. This model predicts the yields and elemental composition of pyrolytic products by means of eight species: tar (represented by a blend of C_6H_6, $C_{10}H_8$ and C_6H_6O), H_2, H_2O, CO, CO_2, CH_4 and dry ash-free char. In this sense, the percentage of each compounds was calculated adjusting the mass balance. The empirical model developed consisting of a system of linear equations, being the main the following equations 1 to 13 [26]:

$$Y_{ch,F} = 0.106 + 2.43 \cdot \exp(-0.66 \cdot 10^{-2} \cdot T) \quad (1)$$

$$Y_{C,ch} = 0.93 - 0.92 \cdot \exp(-0.42 \cdot 10^{-2} \cdot T) \quad (2)$$

$$Y_{O,ch} = 0.07 + 0.85 \cdot \exp(-0.48 \cdot 10^{-2} \cdot T) \quad (3)$$

$$Y_{H,ch} = -0.41 \cdot 10^{-2} + 0.10 \cdot \exp(-0.24 \cdot 10^{-2} \cdot T) \quad (4)$$

$$Y_{H_2,F} = 1.145 \left(1 - \exp\left(-0.11 \cdot 10^{-2} \cdot T\right)\right)^{9.384} \quad (5)$$

$$Y_{CH_4,F} = -2.18 \cdot 10^{-4} + 0.146 \cdot Y_{CO,F} \quad (6)$$

$$Y_{CO,F} = \left(3 \cdot 10^{-4} + \frac{0.0429}{1 + (T/632)^{-7.23}}\right)^{-1} \cdot Y_{H_2,F} \quad (7)$$

$$Y_{C,tar} = (1.05 + 1 \cdot 10^{-4} \cdot T) \cdot Y_{C,bio} \quad (8)$$

$$Y_{O,tar} = (0.92 - 2.2 \cdot 10^{-4} \cdot T) \cdot Y_{O,bio} \quad (9)$$

$$Y_{H,tar} = (0.93 - 3.8 \cdot 10^{-4} \cdot T) \cdot Y_{H,bio} \quad (10)$$

$$Y_{C,F} - Y_{C,ch} \cdot Y_{ch,F} = Y_{C,tar} \cdot Y_{tar,F} + Y_{C,CH_4} \cdot Y_{CH_4,F} + Y_{C,CO} \cdot Y_{CO,F} + Y_{C,CO_2} \cdot Y_{CO_2,F} \quad (11)$$

$$Y_{O,F} - Y_{O,ch} \cdot Y_{ch,F} = Y_{O,tar} \cdot Y_{tar,F} + Y_{O,CH_4} \cdot Y_{CH_4,F} + Y_{O,CO_2} \cdot Y_{CO_2,F} + Y_{O,H_2O} \cdot Y_{H_2O,F} \quad (12)$$

$$Y_{H,F} - Y_{H,ch} \cdot Y_{ch,F} = Y_{H,tar} \cdot Y_{tar,F} + Y_{H,CH_4} \cdot Y_{CH_4,F} + Y_{O,H_2O} \cdot Y_{H_2O,F} \quad (13)$$

where $Y_{ch,F,}$ $Y_{H2,F,}$ $Y_{CO,F,}$ $Y_{H2O,F,}$ $Y_{CO2,F,}$ is the yield of char, H_2, CO, H_2O, CO_2 of pyrolysis process, respectively. $Y_{C,\,bio}$, $Y_{C,\,char}$, $Y_{C,\,tar}$, $Y_{H,\,bio}$, $Y_{H,\,char}$, $Y_{H,\,tar}$, $Y_{O,\,bio}$, $Y_{O,\,char}$, $Y_{H,\,tar}$ is the CHO composition of biomass, char and tar, respectively.

The block R-2 decomposed the char into compounds according to the equation (1), where C represents solid carbon, and S solid sulphur.

$$\text{Char} \rightarrow \text{C} + \text{H}_2 + \text{N}_2 + \text{O}_2 + \text{S} + \text{Ash} \qquad (14)$$

Subsequently, the char oxidation process was modelled in block R-3 to achieve the gasification temperature, obtaining an autothermic gasification process. Finally, the primary gas obtained in the oxidation zone and the residual char were inputs to the R-4 block which represented the process representative of a set of reduction reactions in the gasifier. The air was added to the reactor represented by block R-3, at 1 bar and 25 ºC (stream 5). The air fed rate was 200 L_{NPT}/min and it was constant; this was assumed in order to maintain the reactor hydrodynamics as was performed during the gasification experiments. Processes represented by R-3 and R-4 blocks were simulated using the R-Plug block; this block performs simulation of ideal reactor operated under specific conditions. The real temperature profile and real reactor dimensions (reaction chamber of 0.25 m internal diameter and 2.3 m height) was specified. In addition, the kinetics parameters for each reaction considered were introduced. The reactions involved in gasification process and the kinetic parameters for these reactions are summarized in Tables 4 and 5, respectively. Four models were compared in this work, two were taken from the literature (Martinez-Gonzalez et al. (2018) [27], Champion et al. (2014) [28]) and two models (named Model 1 and Model 2) were developed based on those literature models but by adjusting selected kinetic parameters in order to fit experimental data [28]; the modifications consisted in the adjustment of the pre-exponential factors of selected reactions (Table 5).

Note that among the main assumptions considered, the major simplification of reactor developed herein is the not consideration of hydrodynamics. To quantify potential sources of uncertainty, calculations including volume reduction of reactor (0-75%) to consider the freeboard section, has been carried out. In addition, these calculations were compared with the work of Mohamed et al. [3] where hydrodynamics was considered. The possible absolute error obtained varied between 1.9 and 8 % for CO_2, CH_4, H_2 and CO production.

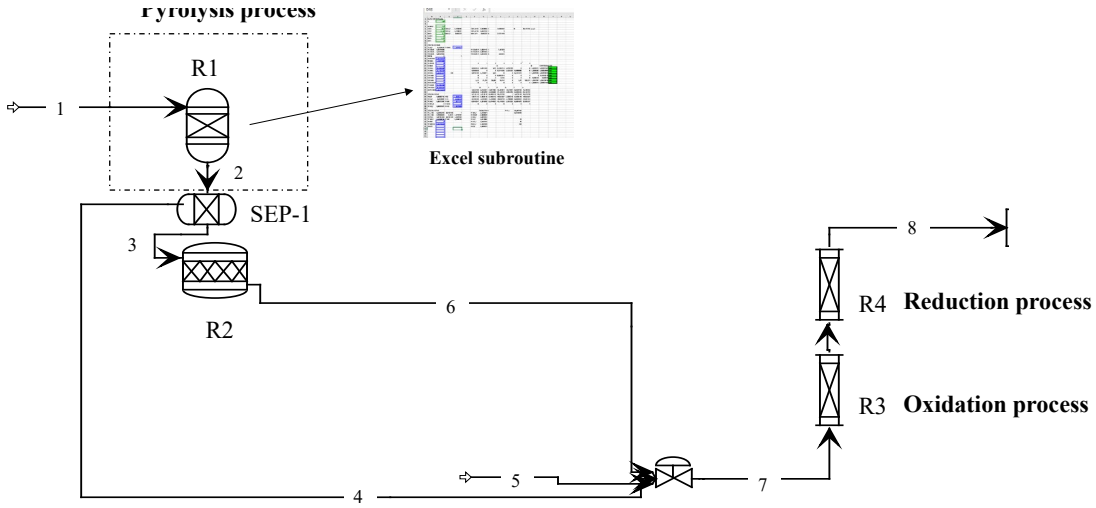

Figure 2. Aspen Plus® flowsheet simulation of the gasification model.

Table 3. Blocks description used in the gasification model.

NAME	*TYPE*	*DESCRIPTION*
R-1	RYIELD	Reactor of biomass pyrolysis, it decomposed the biomass into pyrolytic compounds by means of Excel subroutine. It operated at atmospheric pressure and 700-860 ºC depending on the simulation.
SEP-1	SEP	Separator of char and gas product.

R-2	RSTOIC	The char was separated into its constituent components and ash. It operated at atmospheric pressure and 700-860 ºC depending on the simulation.
R-3	RPLUG	Gasifier. This reactor simulates the oxidation zone of the gasifier. The real temperature profile, real reactor dimensions and kinetic parameters for each reaction were specified. It operated at atmospheric pressure and 700-860 ºC depending on the simulation.
R-4	RPLUG	Gasifier. This reactor simulates the reduction zone of the gasifier. The real temperature profile, real reactor dimensions and kinetic parameters for each reaction were specified. It operated at atmospheric pressure and 700-860 ºC depending on the simulation.

284

Table 4. Chemical reactions and respective kinetic expressions considered in the gasification model.

Process	*Reaction*	*Rate Expression (mol/m³·s)*	*Reference*	*Reaction number*
R-3	Partial oxidation of *C*: $\alpha C(s)+O_2 \rightarrow 2(\alpha-1)\ CO+(2-\alpha)CO_2$	$r=k\cdot T\cdot e^{\frac{-E_a}{RT}}\cdot\frac{6}{dp}[O_2]$ $\alpha=\frac{1+2f}{1+f}$ with $f=4.72\cdot10^{-3}\cdot e^{\frac{37{,}787}{RT}}$	[28, 29]	(1)
	Total oxidation of *CO*: $CO+12O_2 \rightarrow CO2$	$r=k\cdot e^{\frac{-E_a}{RT}}[CO][O_2]^{0.25}[H_2O]^{0.5}$	[7, 30]	(2)
	Partial oxidation of *CH₄*: $CH_4+\frac{1}{2}O_2 \rightarrow CO+2H_2$	$r=k\cdot e^{\frac{-E_a}{RT}}[CH_4]^{0.7}[O_2]^{0.8}$	[28]	(3)
	Hydrogen oxidation: $H_2+\frac{1}{2}O_2 \rightarrow H_2O$	$r=k\cdot e^{\frac{-E_a}{RT}}[H_2]\ [O_2]$	[30]	(4)
	Partial oxidation of phenol: $C_6H_6O+4O_2 \rightarrow 6CO+3H_2O$	$r=k\cdot T\cdot e^{\frac{-E_a}{RT}}[C_6H_6O]^{0.5}[O_2]$	[31]	(5)
	Partial oxidation of benzene: $C_6H_6+\frac{9}{2}O_2 \rightarrow 6CO+3H_2O$	$r=k\cdot T\cdot e^{\frac{-E_a}{RT}}[C_6H_6]^{0.5}[O_2]$	[32]	(6)
R-4	Water Gas: $C+H_2O \rightleftharpoons CO+H_2$	$r=k\cdot e^{\frac{-E_a}{RT}}[C][H_2O]$	[27, 33]	(7)
	Water-gas shift: $CO+H_2O \leftrightharpoons CO_2+H_2$	$r=k\cdot e^{\frac{-E_a}{RT}}\left\langle[CO][H_2O]-\frac{[CO_2][H_2]}{k_{eq}}\right\rangle$ $k_{eq}=0.022\cdot e^{\frac{34{,}730}{RT}}$	[34]	(8)
	Steam reforming: $CH_4+H_2O \rightleftharpoons CO+3H_2$	$r=k\cdot e^{\frac{-E_a}{RT}}[CH_4][H_2O]$	[27, 34]	(9)
	Boudouard: $C+CO_2 \rightleftharpoons 2CO$	$r=k\cdot e^{\frac{-E_a}{RT}}[C]$	[27, 29]	(10)
	$C_6H_6O \rightarrow CO+0.4C_{10}H_8+0.15C_6H_6+0.1CH_4+0.75H_2$	$r=k\cdot e^{\frac{-E_a}{RT}}[C_6H_6O]$	[35, 36]	(11)
	$C_6H_6O+3H_2O \rightarrow 4CO+0.5C_2H_4+1CH_4+3H_2$	$r=k\cdot e^{\frac{-E_a}{RT}}[C_6H_6O]$	[36]	(12)
	$C_{10}H_8 \rightarrow 6.5C+0.5C_6H_6+0.5CH_4+1.5H_2$	$r=k\cdot e^{\frac{-E_a}{RT}}[C_{10}H_8]^{1.6}[H_2]^{-0.5}$	[27, 37]	(13)

Table 5. Kinetic parameters of the main chemical reactions considered in the gasification models used.

Process		***Martinez-Gonzalez et al. (2018)[19]***		***Champion et al. (2014) [20]***		***Model 1 (This work)***		***Model 2 (This work)***	
	Reaction	*k*	E_a *(J/mol)*	*k*	E_a *(J/mol)*	*k*	E_a *(J/mol)*	*k*	E_a *(J/mol)*
R-3	(1)	$3.70 \cdot 10^{10}$	$1.50 \cdot 10^{5}$	$2.98 \cdot 10^{1}$	$1.49 \cdot 10^{5}$	$3.70 \cdot 10^{10}$	$1.50 \cdot 10^{5}$	$3.70 \cdot 10^{10}$	$1.50 \cdot 10^{5}$
	(2)	$3.98 \cdot 10^{20}$	$1.67 \cdot 10^{5}$	$1.78 \cdot 10^{10}$	$1.80 \cdot 10^{5}$	$1.78 \cdot 10^{10}$	$1.80 \cdot 10^{5}$	$1.78 \cdot 10^{10}$	$1.80 \cdot 10^{5}$
	(3)	$2.40 \cdot 10^{11}$	$1.26 \cdot 10^{5}$	$1.58 \cdot 10^{12}$	$2.02 \cdot 10^{5}$	$1.58 \cdot 10^{12}$	$2.02 \cdot 10^{5}$	$1.58 \cdot 10^{12}$	$2.02 \cdot 10^{5}$
	(4)	$2.19 \cdot 10^{18}$	$1.09 \cdot 10^{5}$	$1.08 \cdot 10^{7}$	$1.25 \cdot 10^{5}$	$1.08 \cdot 10^{7}$	$1.25 \cdot 10^{5}$	$1.08 \cdot 10^{7}$	$1.25 \cdot 10^{5}$
	(5)	$6.55 \cdot 10^{2}$	$8{,}02 \cdot 10^{4}$	$6.55 \cdot 10^{2}$	$8.02 \cdot 10^{4}$	$6.55 \cdot 10^{2}$	$8{,}02 \cdot 10^{4}$	$6.55 \cdot 10^{2}$	$8{,}02 \cdot 10^{4}$
	(6)	$2.40 \cdot 10^{11}$	$1.26 \cdot 10^{5}$	$2.4 \cdot 10^{11}$	$1.26 \cdot 10^{5}$	$2.40 \cdot 10^{11}$	$1.26 \cdot 10^{5}$	$2.40 \cdot 10^{11}$	$1.26 \cdot 10^{5}$
R-4	(7)	$2.00 \cdot 10^{5}$	$4.99 \cdot 10^{4}$	$2.39 \cdot 10^{2}$	$1.29 \cdot 10^{5}$	$8.00 \cdot 10^{-3}$	$4.99 \cdot 10^{4}$	$8.00 \cdot 10^{-3}$	$4.99 \cdot 10^{4}$
	(8)	$2.78 \cdot 10^{3}$	$1.26 \cdot 10^{4}$	$2.78 \cdot 10^{-1}$	$1.26 \cdot 10^{4}$	$2.78 \cdot 10^{2}$	$1.26 \cdot 10^{4}$	$2.78 \cdot 10^{1}$	$1.26 \cdot 10^{4}$
	(9)	$3.00 \cdot 10^{8}$	$1.25 \cdot 10^{5}$	$4.92 \cdot 10^{-11}$	$3.66 \cdot 10^{5}$	$3.00 \cdot 10^{13}$	$1.25 \cdot 10^{5}$	$3.00 \cdot 10^{13}$	$1.25 \cdot 10^{5}$
	(10)	$1.05 \cdot 10^{13}$	$1.35 \cdot 10^{5}$	$3.18 \cdot 10^{7}$	$3.68 \cdot 10^{5}$	$1.05 \cdot 10^{13}$	$1.35 \cdot 10^{5}$	$1.05 \cdot 10^{13}$	$1.35 \cdot 10^{5}$
	(11)	$1.00 \cdot 10^{7}$	$1.00 \cdot 10^{5}$	$1.00 \cdot 10^{7}$	$1.00 \cdot 10^{5}$	$1.00 \cdot 10^{7}$	$1.00 \cdot 10^{5}$	$1.00 \cdot 10^{7}$	$1.00 \cdot 10^{5}$
	(12)	-	-	$1.00 \cdot 10^{7}$	$1.00 \cdot 10^{5}$	$1.00 \cdot 10^{7}$	$1.00 \cdot 10^{5}$	$1.00 \cdot 10^{7}$	$1.00 \cdot 10^{5}$
	(13)	$1.00 \cdot 10^{14}$	$3.50 \cdot 10^{5}$	$1.70 \cdot 10^{7}$	$3.50 \cdot 10^{5}$	$1.00 \cdot 10^{14}$	$3.50 \cdot 10^{5}$	$1.00 \cdot 10^{14}$	$3.50 \cdot 10^{5}$

3. Discussion and results

3.1 Kinetic model approach to simulate the gasification process and model calibration

In this section are shown the results of the models of Champion et al. (2014) [28] and Martinez-Gonzalez et al. (2018) [27] and its comparison with experimental results. Then, it is evaluated the influence of kinetic parameters of selected reactions in order to improve the simulation results, and from this analysis it was derived a set of adjusted kinetic parameters that could improve simulation results (Model 1 and Model 2). The experimental results for model calibration are those obtained in the pilot-scale BFB gasification unit using pine pellets, and ER equal to 0.22 (see Table 2) [2].

Figure 3 shows the predicted gas composition given by using the kinetic models of Champion et al. (2014) [28] and Martinez-Gonzalez et al. (2018) [27], and its comparison with the experimental results and respective absolute error. The model developed by Champion et al. (2014) does not give good predictions when compared to the experimental results, overestimating H_2 and CO yields and underestimating CO_2 and N_2 concentration (Figure 3a). By comparison, the model of Martinez-Gonzalez et al. (2018) gives a better prediction when compared to experimental results, despite relevant deviations are observed.

From the analysis made it were observed significant differences between model predictions and experimental results for the producer gas composition. Then, a calibration procedure was implemented on the kinetic parameters of the reactive mechanism, following an approach based on the modification of the pre-exponential factor (k) of the reactions considered in the model. In this procedure, the pre-exponential factor of each chemical reaction considered in the model was modified by using distinct literature values data for the pre-exponential factor, one by one, with the other parameters kept constant. It

318 was observed that by modifying the pre-exponential factor for water-gas shift, water-gas
319 and steam reforming reactions the predicted results of producer gas composition were
320 improved when compared to the experimental results. It is important to state that the
321 distinct pre-exponential factor values used for the reactions under analysis were collected
322 from different bibliography sources and the main aim was to evaluate which one gives a
323 model with better predictions of experimental values obtained in the reactor type and
324 process under study. Thereafter, once calibrated the kinetics of the reactive mechanism
325 adopted in the model using a set of experiment results, a procedure of validation of model
326 results (e.g., for producer gas composition) was made by using a distinct set of
327 experimental results obtained under distinct experimental conditions in the bubbling
328 fluidized bed. That is, the set of experimental conditions and experimental results (e.g.,
329 producer gas composition) used to support the calibration of the model were distinct from
330 those used for model validation. The use of distinct sets of experimental results from the
331 same pilot-scale BFB reactor is considered appropriate because it guarantees the uniformity
332 of other process conditions as reactor design and main hydrodynamics

333 Figure 3a shows the simulation results from Model 1 in comparison with
334 experimental data from Pio et al. (2017) [2]. The deviation between the results of Model 1,
335 and those of Champion et al. (2014), and Martinez-Gonzales et al. (2018), and the
336 experimental data was quantified by using the absolute error, here define as the difference
337 between the simulation value delivered by each model and the experimental value for each
338 gaseous compound considered (CO, CO_2, H_2, CH_4, C_2H_4). Figure 3b displays the total
339 absolute error for each model. It is observed that the simulation results using the model of
340 Champion et al. (2014) are far from experimental results and with significant positive
341 absolute errors namely positive absolute error of 22 % for CO, and 11.5 % for H_2, and
342 negative absolute errors, of 15.1 % for CO_2, 14.64 % for N_2, 2.57 % for CH_4 and 0.19 %

for C_2H_4. In this regard, the model of Martinez-Gonzales et al (2018), offers better predictions for the permanent gas concentrations, showing only significant over-prediction for H_2 (absolute error equal to 5.9 %) and under-predicting N_2 (absolute error equal to 9.2 %). As expected, Model 1 gives best predictions than models of Champion et al. (2014), and Martinez-Gonzales et al. (2018), due to the adjustment of reactions kinetic parameters.

However, thermal degradation kinetics, reactivity, and product characteristics are recognised as influenced also by the type of biomass and operating parameters of the process. Thus, to validate the kinetic fit and check the versatility Model 1, the model must be validated with several biomasses [5], and this is evaluated in Section 3.2.

The model developed in this study has the potential to simulate the gasification process using other gasification agents, e.g. air-steam or steam gasification, because the main reactions as water gas, water-gas shift and steam reforming are considered. However, for those conditions it must be considered a step of model calibration and validation for specific kinetic parameters, as it was made in the present work for air gasification

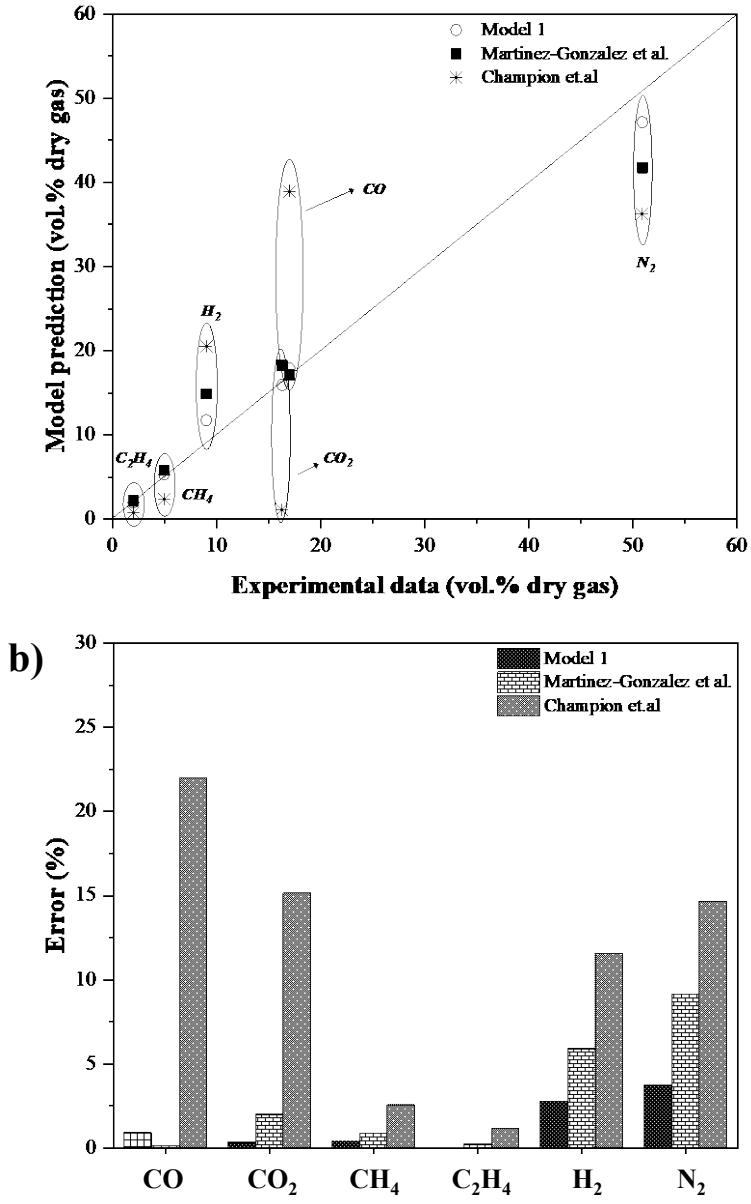

Figure 3. Comparison of simulation results from the kinetic models from literature (Champion et al. (2014) [28], and Martinez-Gonzalez et al. (2018)) [27], Model 1 proposed in this work, and experimental data for pine pellets gasification with ER of 0.22 and bed temperature of 816ºC (±17ºC) [2] a) Concentration of gas compounds; b) Absolute error.

366 3.2 Validation of Model 1

367 Having calibrated the kinetic model with experimental results and suggested an
368 alternative kinetic model, called as Model 1, it was evaluated the model validity
369 considering the gasification of other biomass types and keeping ER constant (ER=0.22),
370 using the same experimental autothermal pilot-scale BFB gasifier [2].

371 The biomass types studied are distinct considering its origin, namely pine or
372 eucalyptus residual biomass, particle size, shape and density, because some samples are
373 chipped and other are pelletized, and this can influence the biomass/char reactivity. In the
374 case of pine pellets, the particle size was the 15-20 mm of length and 6 mm diameter, while
375 the eucalyptus and pine RFB are chipped material with particle size in range 5 mm to 10
376 mm, respectively.

377 Figure 4.a) shows the comparison between the experimental results and Model 1
378 predictions for the operating conditions and biomass types considered. It is observed that
379 the model predicted CO, CO_2, CH_4 and C_2H_4 with higher accuracy than H_2 and N_2. These
380 variations can be attributed to the water-gas shift and water-gas reactions since they were
381 observed as the more influential reactions.

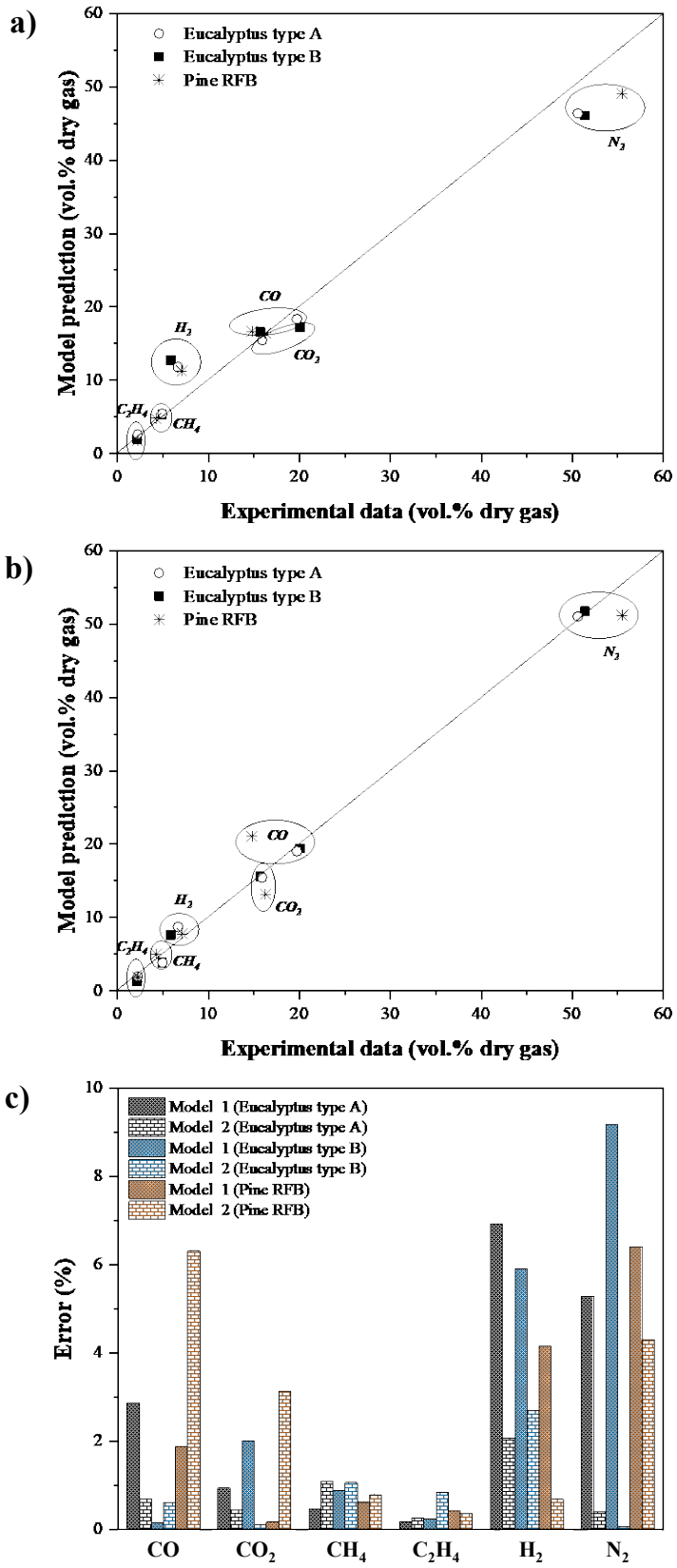

382

383 **Figure 4.** Comparison between experimental results and models predictions for the

384 gasification of eucalyptus type A and B, and pine RFB (ER=0.22): a) Model 1, b) Model

385 2, c) Comparison between absolute error obtained between experimental results and
386 predicted concentration of gaseous species using Model 1 and Model 2.

387 In a first instance, the water-gas reaction should be the main reaction directly
388 affected by biomass characteristics, because it is a solid-gas reaction. Thus, the higher the
389 char reactivity the higher the concentration of H_2 generated should be. However, this trend
390 was not observed, because the biomass with the highest char reactivity presented the lower
391 H_2 yield. Moreover, Pio et al. (2017) [2], Kim et al. (2013) [38] and Lim et al. (2008) [39]
392 also observed the same trend as that offered by Model 1 and for the same types of biomass.
393 Pio et al. (2017) [2] suggested that other phenomenon should be taken into account, such
394 as the pelletized form of particles instead of the chipped form, the former being less reactive
395 and promoting higher char concentration inside the bed. On the other hand, Kim et al.
396 (2013) [38] explained that the water gas-shift reaction contributed significantly in the
397 gasification process. Thus, regarding the conclusions from these studies and following Bell
398 et al. (2010) [40] and Speight (2019) [41] , the water-gas shift reaction can play an
399 important role, and although all chemical species are in gaseous state, the reaction can be
400 considered heterogeneous insofar as the chemistry occurs at the surface of the raw material
401 and the reaction is essentially catalysed by carbon surfaces.

402 Therefore, to account for this effect, a new model approach is suggested, Model 2
403 (Tables 3 and 4), where the water-gas shift reaction kinetics were adjusted to slow down
404 the reaction, and thus, to improve the model predictions accuracy. The pre-exponential
405 factor of the water-gas shift reaction was modified from 278 (for Model 1) to 27.8 (for
406 Model 2), respectively.

407 The simulation results obtained with Model 2 are shown in Figure 4.b). It is
408 observed that the model predictions for gas composition from gasification of Eucalyptus
409 type A and B become improved with Model 2, with a much lower absolute error when

410 compared to Model 1 (Figure 4.c). Nonetheless, this improvement in gas composition
411 predictions is not observed in the case of RFB from pine, where the concentration of H_2
412 was better predicted by Model 1, and also for CO and CO_2 the absolute error between
413 Model 2 predictions and experimental results it too high. Figure 4.c) shows that Model 2
414 predictions are more suitable for samples Eucalyptus A and B, while similar errors were
415 obtained with both models for pine RFB, being slightly lower for Model 1.

416 Thus, it can be concluded that the influence of the water-gas shift reaction and
417 particle size can be relevant subjects to be considered in the simulation of biomass
418 gasification. From the results obtained, there are some indications that for higher biomass
419 particles sizes (e.g., between 10 and 20 mm) better predictions can be obtained by Model
420 1, because it considers a stronger effect of the catalytic activity of the char over the water-
421 gas shift reaction, whereas for smaller particle sizes (e.g., below 10 mm) Model 2 offers
422 better predictions, because in this case the concentration of char inside the bed is lower and
423 thus the contribution of the water-gas shift reaction becomes lower.

424 Besides the characteristics of biomass, other operating parameters as the ER and
425 temperature are of major relevance. The influence of these parameters of gas composition
426 are analysed in sections 3.2.1. and 3.2.2. for the simulations using Model 1 and Model 2.
427

428 3.2.1. Effect of Equivalence Ratio

429 The equivalence ratio (ER) is one of the main variables in direct (air) biomass
430 gasification processes. A low ER will turn the process approaching pyrolysis, whereas a
431 high ER causes biomass combustion. According to Kuo et al. the appropriate ER for
432 biomass gasification is in the range of 0.2-0.35 [42], which was the range used in this study.

433 Thus, to check the robustness of the Aspen Plus® models, it was made a comparison
434 between the simulation results for gasification of different biomass types and ER and a set
435 of experimental results (see Table 2). Figures 7, 8, 9 and 10 show the simulation results
436 compared with experimental data (Pio et al. (2017) [2]) for the product gas composition
437 from gasification of pine pellets, eucalyptus type A, eucalyptus type B and pine RFB as a
438 function of ER, respectively. Table 6 shows the residual solid char predicted by the models
439 for all biomasses; for the experimental information used no data on char concentration are
440 available for comparison. It can be observed that in general, the proposed models fitted the
441 data very close. Moreover, the ER strongly influences the type of gasification products. An
442 increase of ER means that more O_2 is available for oxidation reactions, leading to a
443 decrease in CO, H_2, CH_4 and C_2H_4 and increase in CO_2. The same reason explains that an
444 increase in ER promotes a rise in temperature (Table 2) and a drop in char concentration
445 (Table 6). However, it can be noted, that while the H_2, CH_4 and C_2H_4 concentrations are
446 clearly influenced by the ER and follow the trend shown by experimental results for all
447 biomass studied, the simulated concentrations of CO and CO_2 reflected a minor influence
448 of the ER, although following the trend shown by the experimental results. This can be
449 attributed to the fact that the increase in CO_2 production in combustion zone is consumed
450 by reacting with char in the gasification zone to produce CO. These results are in
451 accordance with results reported in the literature [7, 43].

452 Regarding the model predictions, in the case of pine pellets (Figure 5), the CO_2,
453 CH_4 and C_2H_4 gases were the gases predicted with higher accuracy, with only a slight
454 deviation between experimental and simulated data. Whereas the H_2 gas was predicted with
455 the lowest accuracy, and this can be attributed to the experimental data not following a
456 clear trend. Despite that, the highest absolute error (3 %) obtained for H_2 was found for the
457 experiment whose ER was 0.22. Likewise, the model prediction revealed that the higher

458 the ER the lower the H_2 yield was, which can be attributed to an increase in the ER leading
459 to higher the O/C ratio, thus more oxygen was available, favouring the oxidation reaction
460 [2, 7], as explained before. These results are in accordance with data reported in literature
461 [37].

462 Concerning RFB from Eucalyptus Type A (Figure 6), the model describes reasonably the
463 influence of ER on the concentration of gaseous species, following the same trend as that
464 observed for pine pellets. In addition, the error concerning differences between
465 concentration values predicted and measured is very low for most gases. However, the
466 model overestimates the concentration of H_2 and underestimates the concentration of CH_4,
467 for all ER studied. Typically, the model overestimates the concentration of H_2 in the
468 producer gas, when compared to the experimental results. Among the reasoning that can
469 explain this result can be an overestimation of the relevance of the water-gas shift reaction,
470 and its kinetics parameters must be further improved. However, that specific subject was
471 not analysed in detail in the present work, and must be further studied in future works. In
472 fact, it has been reported [6] that chemical equilibrium simulation of producer gas
473 composition also delivers overestimations of the concentration of H_2 when compared to
474 experimental results.

475 Figure 7 shows the comparison between the gas composition obtained with the
476 simulation model and experimental results from the pilot plant for eucalyptus type B, for
477 different ER. Note that for ER higher than 0.3 (conditions with lower biomass feed rate),
478 the model fails to give good predictions of the gas composition, together with prediction
479 of the existence of O_2 in the gas product. This effect was more notable for CO and CO_2
480 concentrations, where the model results deviation from experimental results leads to a
481 change in the trend of the gas composition with ER. Furthermore, H_2 was not predicted
482 with accuracy in all range of ER studied and the predicted concentration followed a distinct

trend from that observed in the experimental results; the higher the ER the lower the H_2 concentration predicted, while the experimental results showed the reverse trend. Similar to that observed for gasification of Eucalyptus type A, the CH_4 was underestimated and the H_2 was overestimated.

Regarding RFB from pine (Figure 8), it can be observed that the model predictions, that is in good agreement with the experimental results. However, in the same way as before, the predicted H_2 concentration was overestimated, and shows the highest absolute error prediction.

Table 6 also shows the carbon conversion efficiency (CCE) for both experimental and predicted (model) results, which was calculated according to Eq (15), as the ratio between the mass of carbon present in the gaseous compounds in the produced dry gas and the mass of carbon present in the solid fuel fed to the reactor. The CCE is a commonly used parameter in gasification process to deliver the fraction of carbon in the solid fuel that was converted to permanent gases (CO, CO_2, CH_4, light hydrocarbons) containing carbon. The experimental results show lower values of CCE than the Model 1 predictions, but higher values than Model 2 predictions. Moreover, a tendency for the increase in CCE with ER was observed for both experimental [2] and model results, as explained by an increasing degree of solid fuel conversion to light gases containing carbon (e.g., CO_2, CO) in result of the higher availability of O_2 with increasing ER.

$$CCE(\%) = \frac{V_G \cdot \frac{P_G}{R \cdot T_G} \cdot M_C \cdot \sum_i \varepsilon C_i \cdot y_i}{m_F \cdot w_{CF}} \cdot 100 \qquad (15)$$

where V_G is the volumetric gas flow rate (Nm^3/s) of the dry gas produced, P_G and T_G are the absolute pressure (Pa) and absolute temperature (k) of dry gas, R is the ideal gas constant (8.314J/(mol K)), M_C is the molar mass of carbon, index i means gaseous compound (e.g., CO, CO_2, CH_4, C_2H_4) Ɛci is the molar fraction of carbon in gaseous

compounds containing carbon ($\varepsilon_{c,CO2}$=1, $\varepsilon_{c,CO}$=1, $\varepsilon_{c,CH4}$=1 and $\varepsilon_{c,C2H4}$=2), y_i is the molar fraction of CO_2, CO CH_4, and C_2H_4 in the dry gas produced, m_F is the biomass mass flow rate (kg $_{dry\ basis}$/s) adn w_{FC} is the mass fraction of carbon in the biomass (kg_C/kg $_{biomass\ dry\ basis}$).

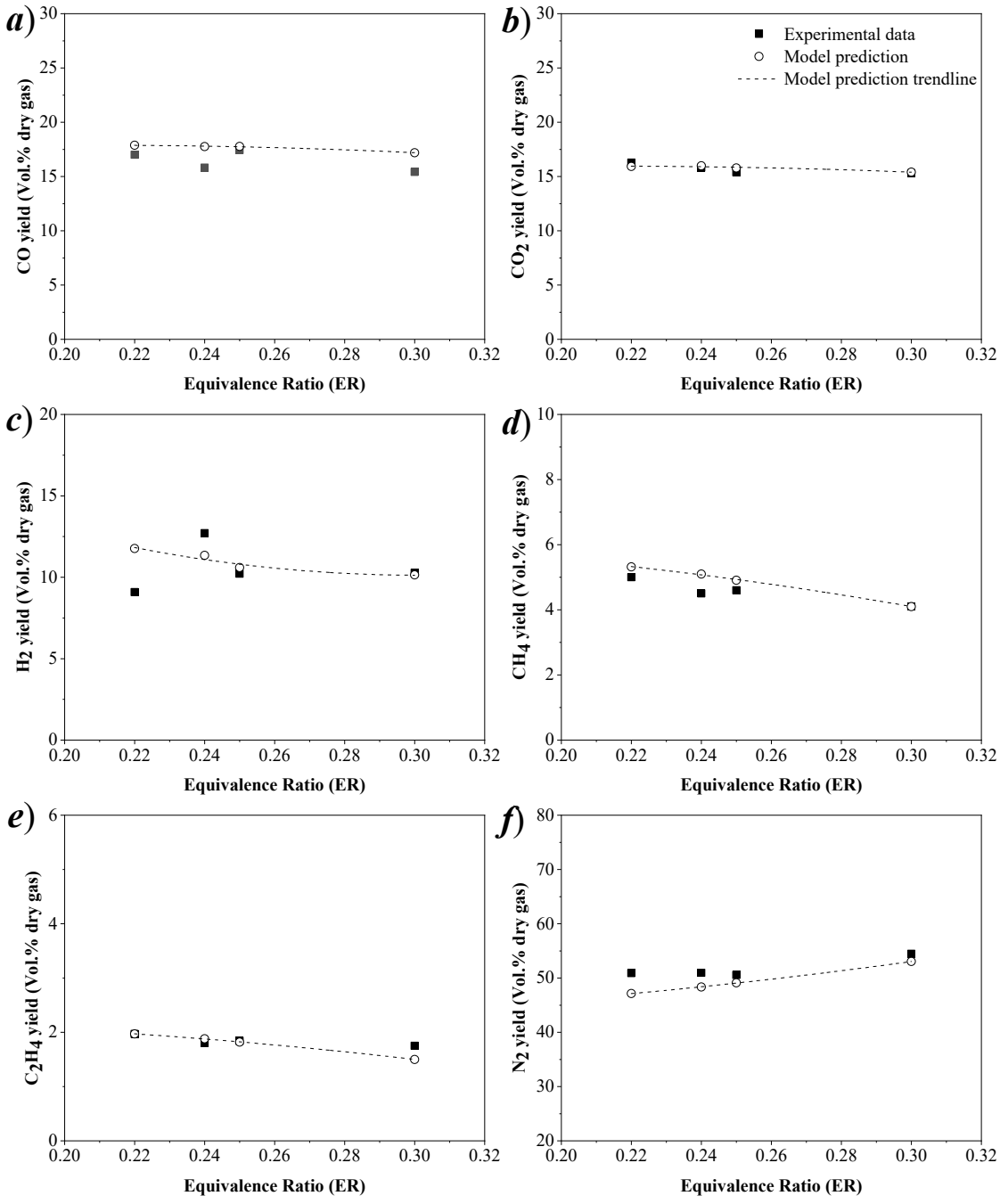

513 **Figure 5.** Comparison between the gas composition (vol.% dry gas) obtained with the
514 simulation Model 1 and experimental results from gasification of pine pellet biomass
515 with different ER, in the pilot-scale reactor [2].

516

517

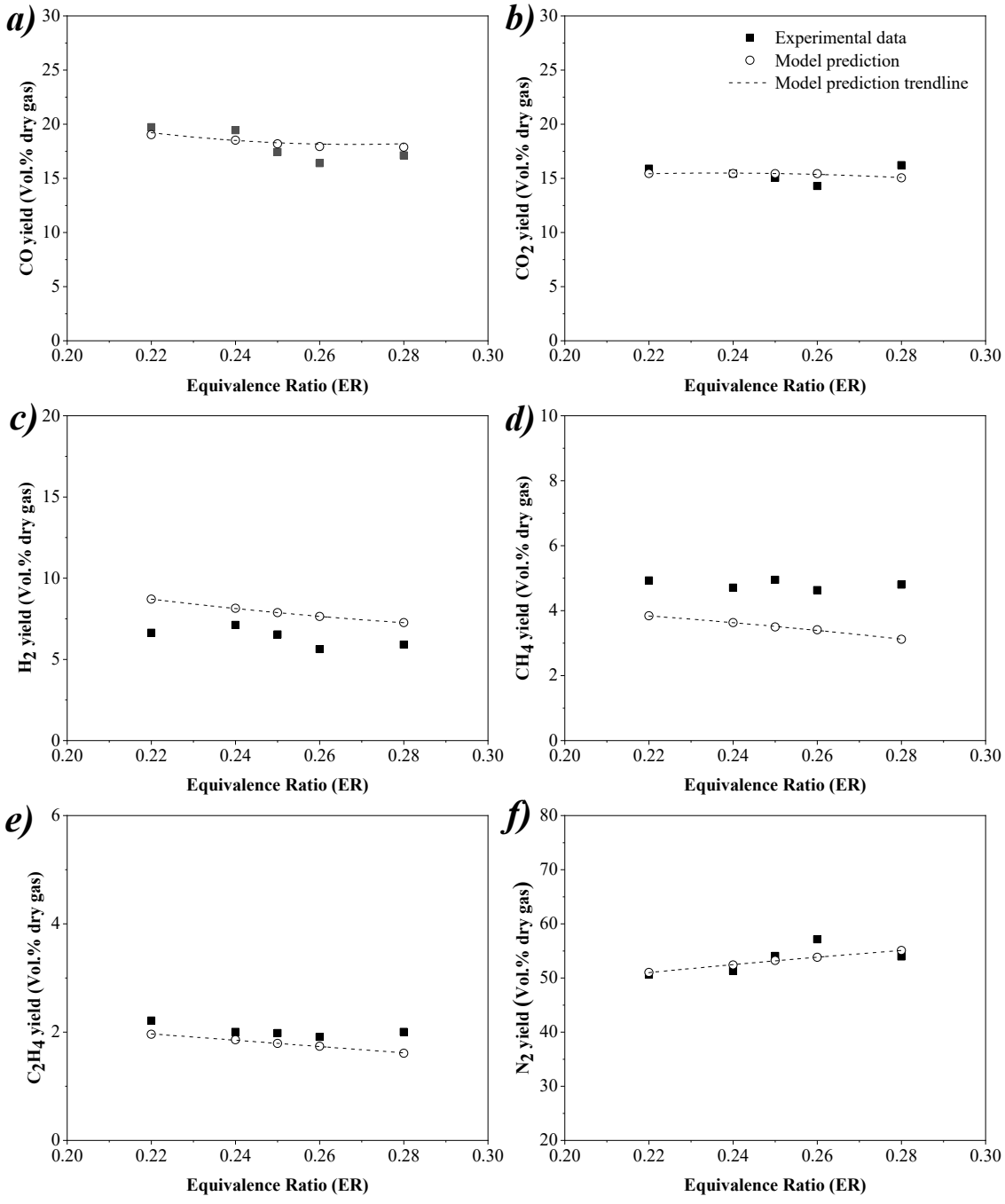

518

Figure 6. Comparison between the gas composition (vol.% dry gas) obtained with the simulation Model 2 and experimental results from gasification of eucalyptus type A with different ER, in the pilot-scale reactor [2].

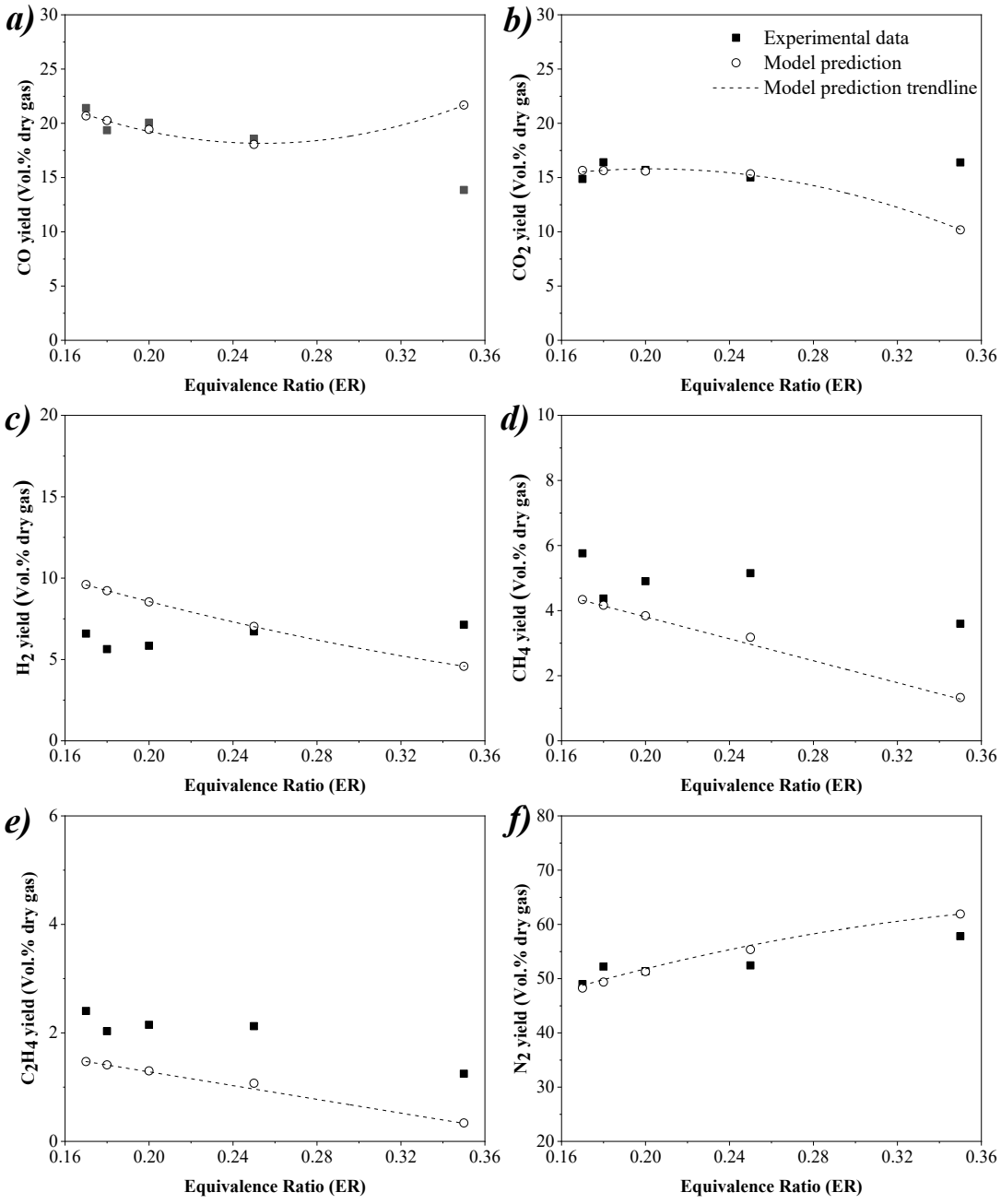

Figure 7. Comparison between the gas composition (vol.% dry gas) obtained with the simulation Model 2 and experimental results from gasification of eucalyptus type B with different ER in the pilot-scale reactor [2].

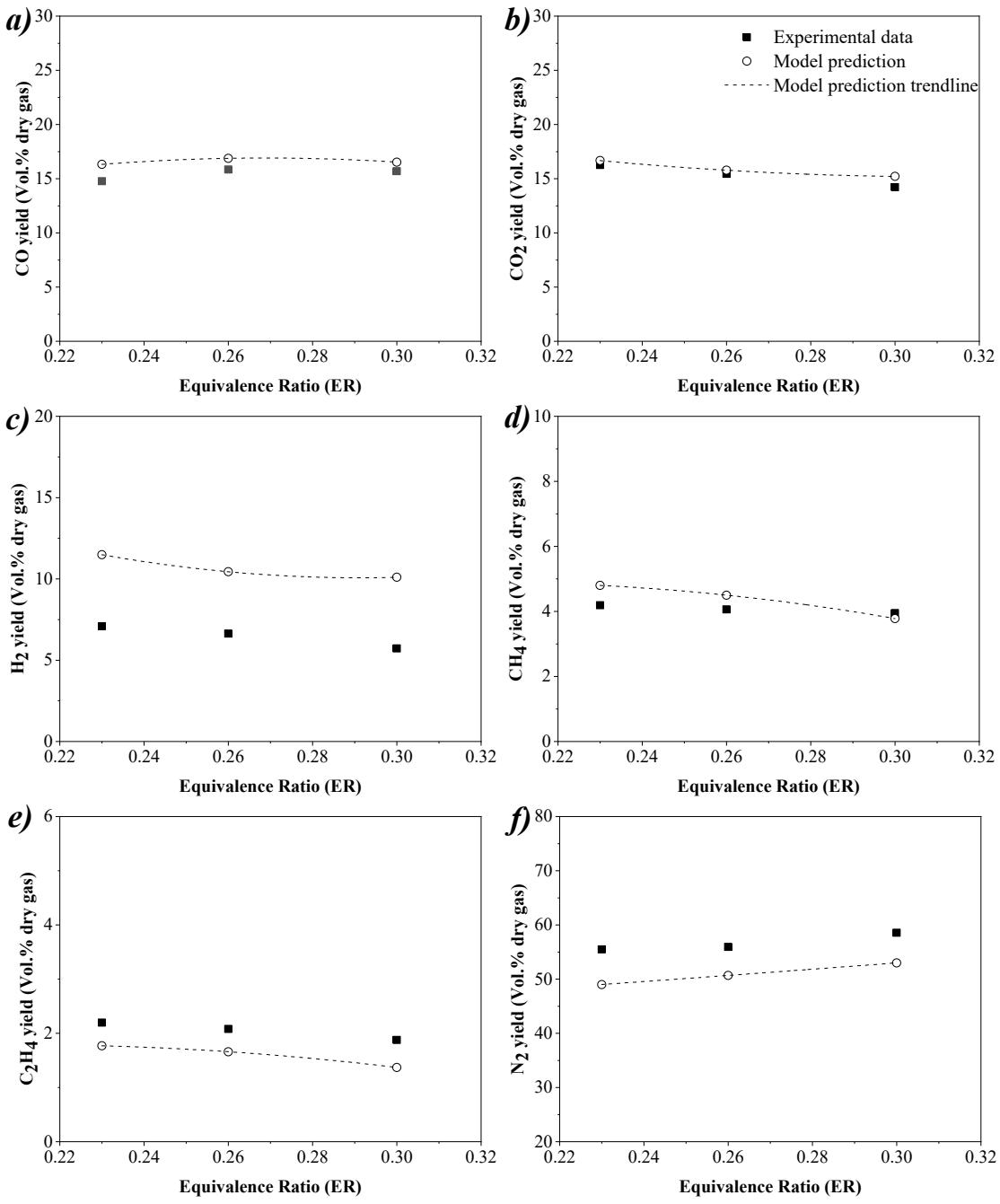

Figure 8. Comparison between the gas composition (vol. % dry gas) obtained with the simulation Model 2 and experimental results from gasification of pine RFB with different ER, in the pilot-scale reactor [2].

535

536 **Table 6**. Char concentration predicted during gasification of the biomass types studied
537 and carbon conversion efficiency (CCE) for experimental results and model predictions.

	Equivalence ratio (ER)	*Average bed Temperature (ºC)*	*Char (wt.%)*	*CCE (%)*	
				Experimental data	*Model data*
Pine pellet	0.22	816 ±17	2.13	69.49	70.14
	0.24	802 ±04	1.32	70.75	75.51
	0.25	854 ±06	0.81	78.85	80.78
	0.30	833 ±02	0.00	77.52	80.33
Eucalyptus type A	0.22	804 ±07	2.54	77.09	72.86
	0.24	798 ±08	1.53	79.90	75.98
	0.25	812 ±05	0.80	75.49	73.54
	0.26	810 ±09	0.30	70.78	73.16
	0.28	818 ±03	0.00	85.79	80.07
Eucalyptus type B	0.17	736 ±19	4.82	63.57	59.27
	0.18	709 ±14	4.26	59.99	58.18
	0.20	719 ±21	2.93	69.91	64.65
	0.25	800 ±05	0.00	83.62	74.68
	0.35	813 ±14	0.00	87.54	80.80
Pine RFB	0.23	786 ±12	0.34	65.55	68.06
	0.26	811 ±03	0.00	68.82	70.17
	0.30	830 ±02	0.00	71.35	71.47

538

539 3.2.2 Effect of temperature

540 In this section, it is analysed the accuracy of Model 2 results versus the gasification
541 temperature. As noted above, the gasifier temperature increased with ER. Thus, the
542 operating bed temperature is also a key parameter in direct gasification to optimize the
543 producer gas quality because the gasification reactions are mostly endothermic. In general,
544 and accordingly to Le Chatelier`s principle, high temperatures favour the endothermic
545 reaction, while exothermic reactions are benefitted at low temperatures.

546 In this respect, the proposed model was validated for the four biomasses studied as
547 a function of gasification temperature. In the proposed validation, the results from the

548 fluidized bed gasifier are relative to bed temperatures in the range of 700-860 ºC. Figures
549 9, 10, 11 and 12 show the comparison of model predictions and experimental results for
550 the dry gas composition at different temperatures, and implicitly at distinct ER (see Table
551 2 for entries relative to ER and temperature), for pine pellet, eucalyptus type A, eucalyptus
552 type B and pine RFB, respectively. For the bed temperature range studied, the simulated
553 gas compositions are in good agreement with the experimental data for all biomasses.

554 Regarding pine pellet biomass (Figure 9), it can be observed that the overall trend
555 of the producer gas composition predicted by the model was similar to experimental results.
556 The highest deviations of the results are obtained for H_2 yield. In addition, no clear
557 influence of the temperature in the concentration of the different gases monitored is
558 observed; the concentration shows only slight variations with temperature. This fact can be
559 owing to variation in temperature between experiments being not large enough to see
560 differences.

561 For its part, the present simulation results for the eucalyptus type A (Figure 10),
562 were in good agreement with the experimental data. The highest deviations were obtained
563 for H_2 and CH_4 which were overestimated and underestimated, respectively. Likewise, the
564 concentration of the gases analysed did not present any clear trend as function of the
565 temperature, and this can be explained by the narrow range of temperatures used (typically
566 within a range with an amplitude lower than 100ºC).

567 In the case of eucalyptus type B (Figure 11), the agreement between simulation
568 results and experimental data depends on the operating conditions and the gas species
569 considered. With exception of the CO concentration in the whole temperature range and
570 CO_2 concentration in the lower temperature range, the model results show significant
571 differences relative to the experimental results. For the lower temperature range, there is

572 little influence of the temperature on the concentration of the several gas species studied,
573 despite a slight trend to an increase in CO, CH_4, C_2H_4 and H_2 concentration with
574 temperature can be observed in some circumstances; on the other hand, the experimental
575 values of concentration of CO, CH_4, C_2H_4 and H_2 show a trend to increase, whereas that of
576 CO tends to decrease. It must be noted that the concentration of char in the reactor bottom
577 bed predicted by the model also decreases from 5 to 0 wt.% (Table 6). Thus, this behaviour
578 may be explained by the fact that the Boudouard reaction and water gas reaction, are both
579 endothermic, and an increase in temperature promotes an increase in the products
580 generation, whereas, the water-gas shift reaction is exothermic, thus it is favoured at low
581 temperatures. Therefore, the trade-off between reactions can explain the behaviour
582 observed, as the increase of H_2 and CO concentration with the temperature in the lower
583 temperature range. However, as explained before, the rise of bed temperature was resulting
584 from an increase in ER, thus, more oxygen was available, favouring the oxidation reactions,
585 and consequently the decrease of combustible gases such as CH_4, C_2H_4, CO or H_2.
586 However, the model did not predict the corresponding increase on CO_2 concentration,
587 although the experimental results show an increase. This subject must be further analysed
588 in order to understand the true effect of the trade-off between the set of reactions involved.

589 Concerning the pine RFB (Figure 12), the predicted concentration in the producer
590 gas of various gaseous compounds is in good agreement with the experimental data, except
591 for H_2 and C_2H_4; the maximum absolute error in predicting experimental values was
592 obtained for H_2, namely 4.5%. The model results agree with experimental results
593 concerning the influence of temperature on producer gas composition. Nevertheless, there
594 is only a slight influence of temperature on the concentration of the gas species considered,
595 as also observed in the experimental results.

596

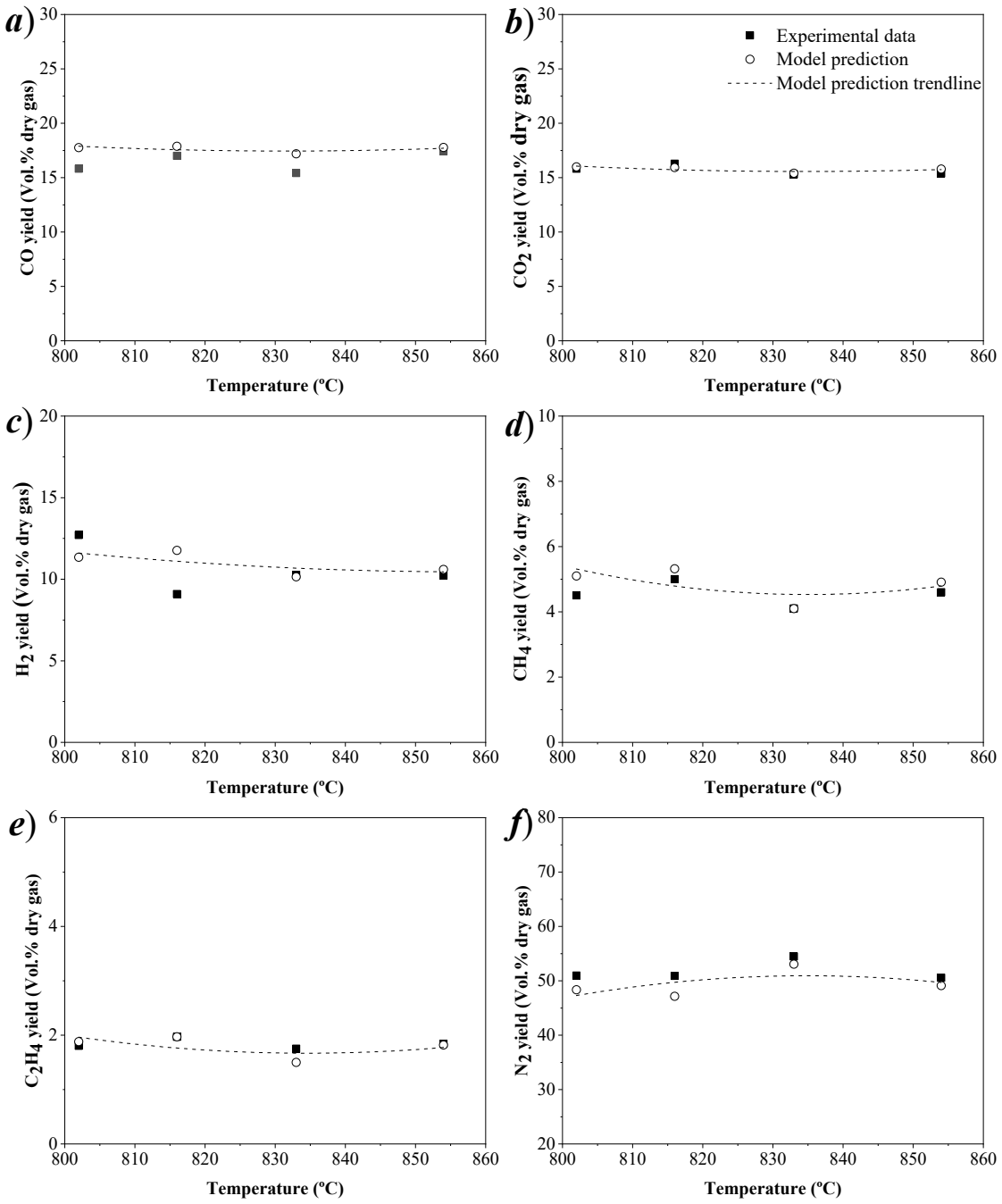

Figure 9. Comparison between the gas composition (vol.% dry gas) obtained with the simulation Model 2 and experimental results from gasification of pine pellet for different temperatures, in the pilot-scale reactor [2].

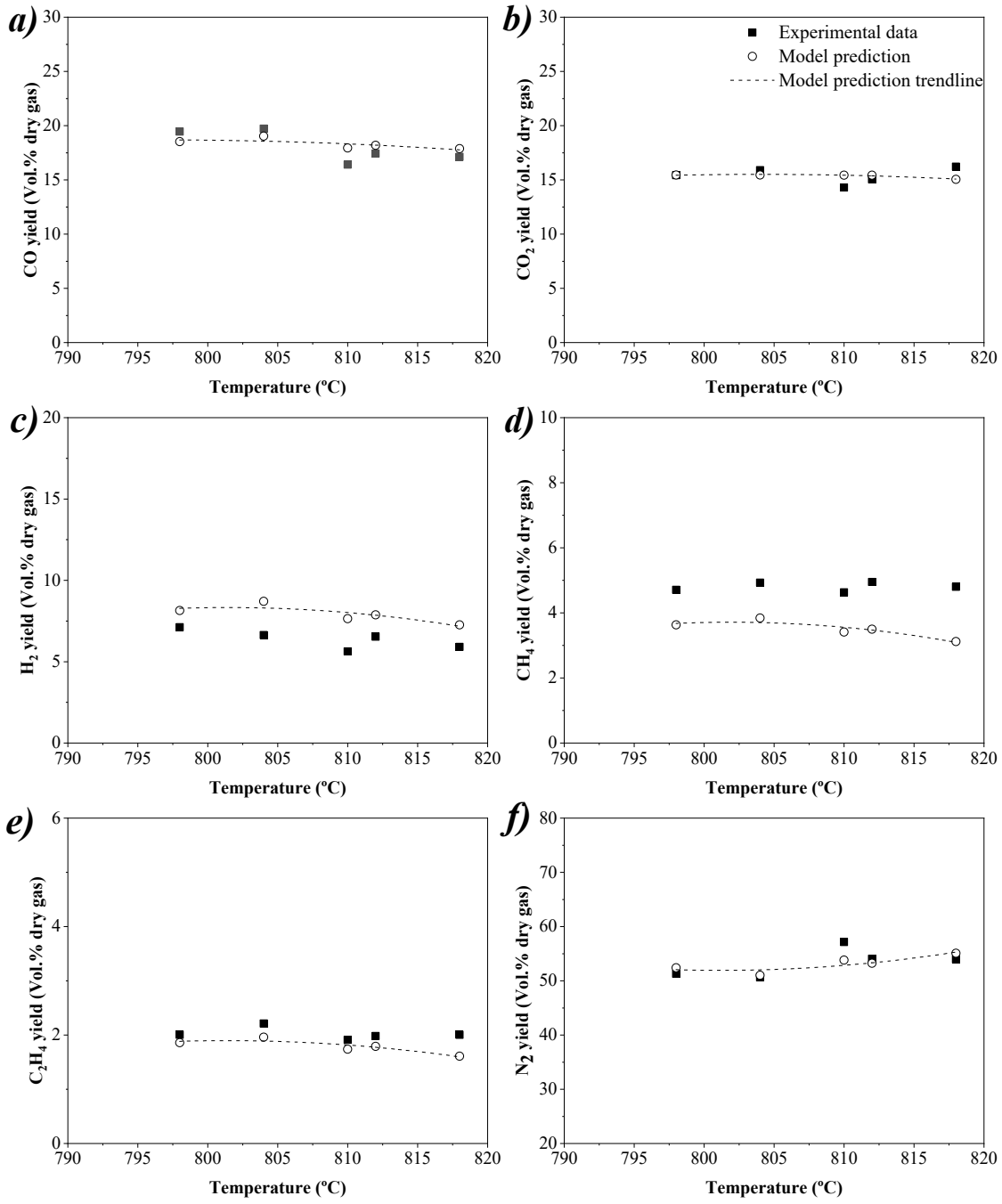

Figure 10. Comparison between the gas composition (vol.% dry gas) obtained with the simulation Model 2 and experimental results from gasification of eucalyptus type A biomass for different temperatures, in the pilot-scale reactor [2].

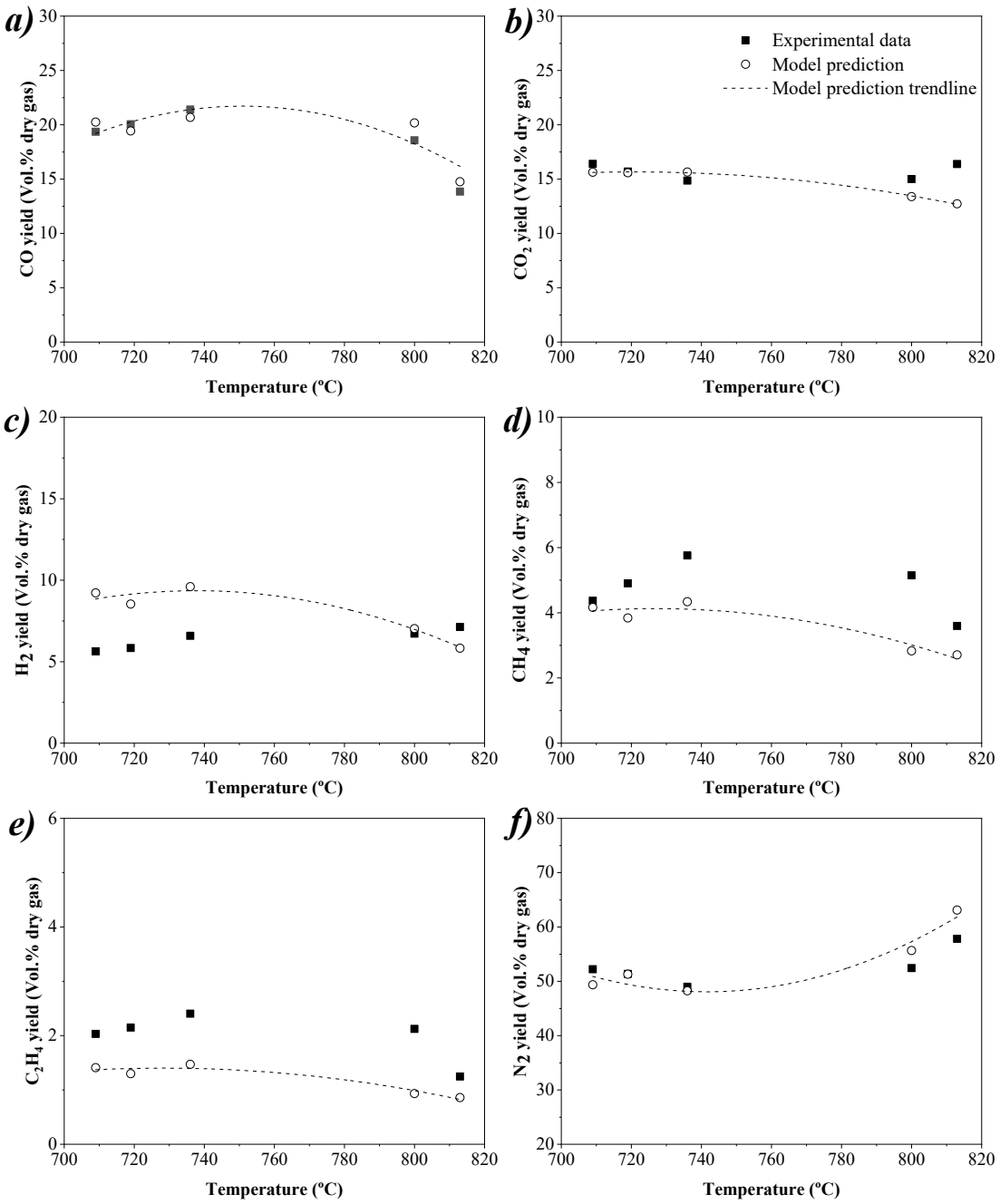

Figure 11. Comparison between the gas composition (vol % dry gas) obtained with the simulation Model 2 and experimental results from gasification of eucalyptus type B biomass for different temperatures, in the pilot-scale reactor [2].

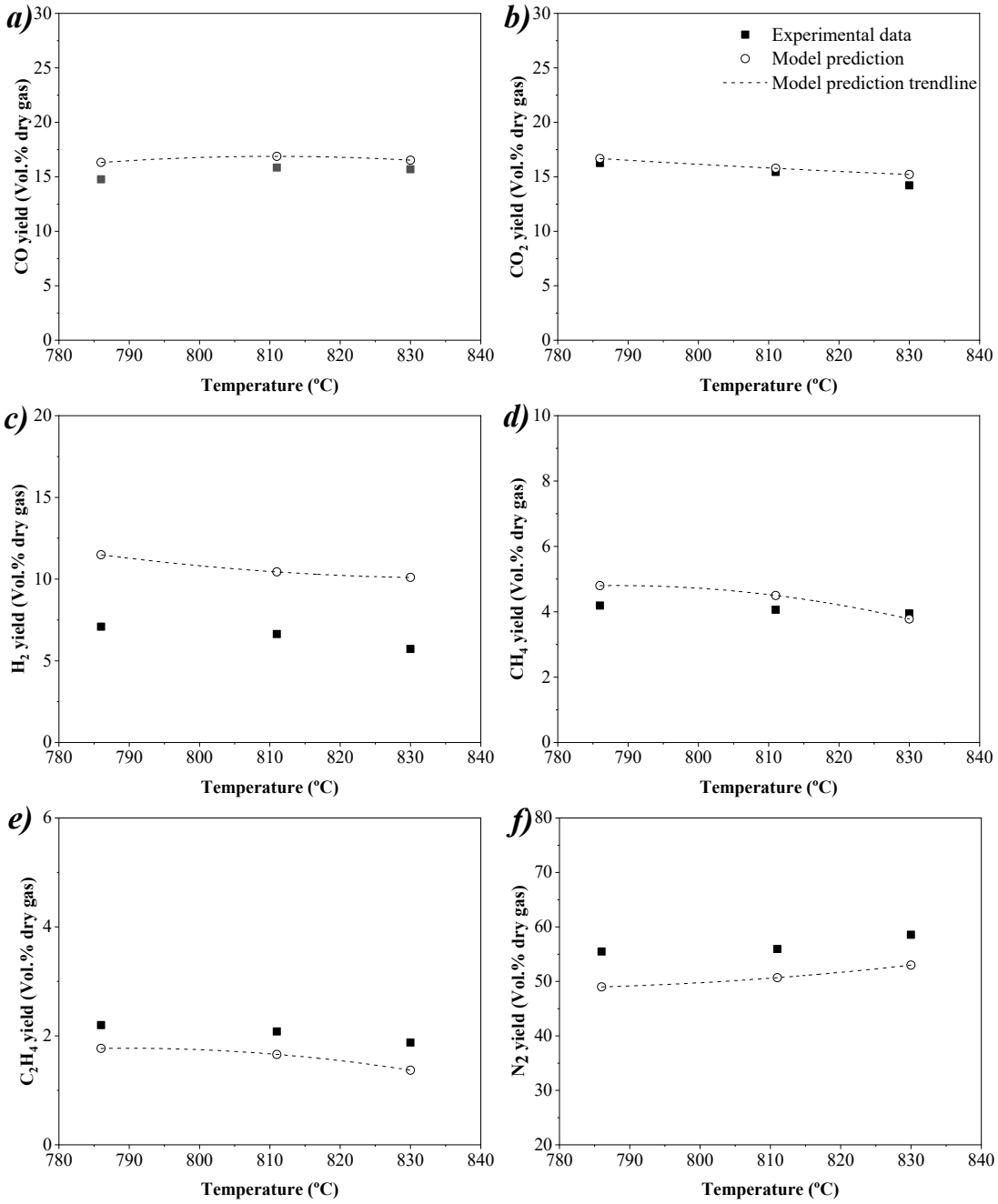

Figure 12. Comparison between the gas composition (vol % dry basis) obtained with the simulation Model 2 and experimental results from gasification of RFB from pine for different temperatures, in the pilot-scale reactor [2].

3.2 Effect of ER and bed temperature on tar formation

One of the main technical barriers and problems related to biomass gasification is the presence of tar in the producer gas. Therefore, it is of vital importance to have good model predictions and experimental results relating tar formation. Nonetheless, despite several technologies for tar quantification [4], it is often difficult and expensive to properly quantify the tar in producer gas. At this stage, the numerical simulation could be a first approach to predict the tar concentration in the producer gas; nevertheless, the models need to be previously calibrated and validated.

In this context, considering the reasonable agreement between model results and experimental data for several gaseous compounds as CO, CO_2, CH_4, C_2H_4, CO or H_2, it was opted to use the Aspen Plus model to simulate the tar concentration in the producer gas under the gasification conditions analysed; however, it is not possible at this stage to calibrate and validate the model with experimental results from the gasification experiments in the pilot-scale fluidized bed, because that was not experimentally monitored. Figure 13 shows the predicted tar concentration in the producer gas as a function of ER and temperature for the conditions of the gasification experiments made in the pilot-scale reactor (Table 2). The predicted tar concentration was between 20 and 42 g/Nm^3, which is in accordance with tar concentration results reported in the literature regarding biomass gasification [3, 18, 43-45]. An increase in the ER shows a beneficial effect on reducing tar concentration, which can be explained in result of an increase in oxygen availability to react with it. The simulation results also show that the increase in temperature promotes a decrease in tar concentration, and this can be explained as resulting from tar destruction reactions, as the partial oxidation or cracking reactions shown in Table 4. During eucalyptus type B gasification (biomass studied for a wider range of ER) the predicted tar concentration showed a decreasing trend from 42 to 25 g/Nm^3 with the increase of ER from 0.17 to 0.35.

For similar values of ER, the predicted tar concentration during gasification of eucalyptus type A and B was higher than for pine pellet and RFB from pine, which can be associated with the characteristics of the biomass, that are model inputs; for example, a higher content of volatile matter in the biomass can results in an increase in tar concentration [46]. However, considering that the volatile matter content (around 69-78 wt.% dry basis) of the biomass types studied was not so different, perhaps other factors come into play to justify the differences in tar concentration predicted, as for example the particle size. According to Mani et al. and Kang et al. [47, 48], this fact could be attributed to smaller particles have larger surface are leading to less diffusion resistance and better heat transfer, favouring the production of tar due to the complete biomass pyrolysis. On the contrary, when larger particle sizes are used, the reactions in the pyrolysis zone of the gasifier are weaker than those of the smaller particle sizes. Therefore, pyrolysis is not complete, resulting in a low tar yield. Similar results have been reported by Yin et al., [49] who detected during the peach pruning gasification a decreasing trend from 550 to 14.43 mg/Nm^3 as the particle size increased from 1 to 6-8 cm. Finally, the tar concentration in the producer gas for all biomasses and operating conditions studied herein, significantly exceeded the standard for use in various industrial applications, such as fuel cells (1 mg/Nm^3), compressors (50 to 500 mg/Nm^3), internal combustion engines (50 mg/Nm^3) and gas turbines (5 mg/Nm^3) [50].

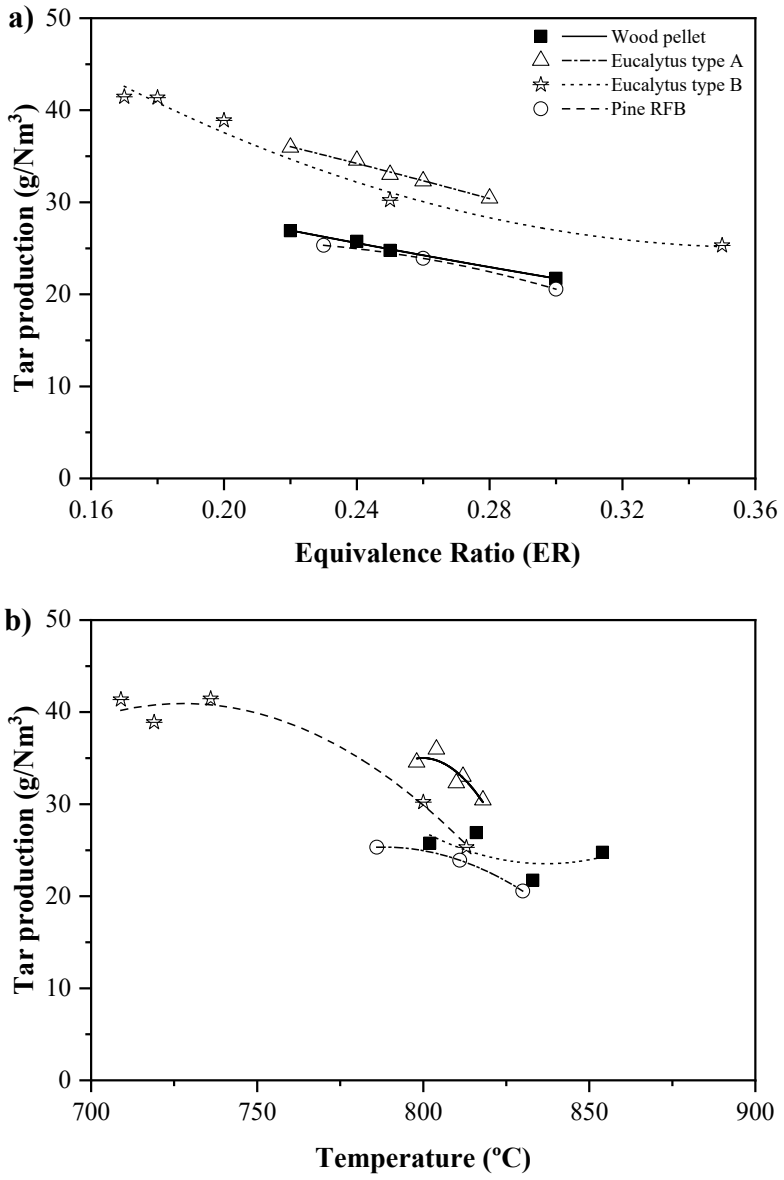

669

670 **Figure 13.** Model predictions of tar concentration in the producer gas during gasification
671 of the biomass types studied (conditions of Table 2): a) Effect of equivalence ratio and b)
672 effect of temperature.

673

674 **4. Conclusions**

675 In this work, direct (air) biomass gasification in a bubbling fluidized bed reactor was
676 simulated using Aspen Plus®. A kinetic mechanism, including the main solid and gaseous
677 compounds, including also tar, typical of biomass gasification was used to simulate the

process. It was evaluated how the kinetic mechanism with parameters from the literature could describe experimental results obtained in a pilot-scale fluidized bed reactor, and how adjustment of specific kinetic parameters of some reactions could improve the predictions of the model, using a model calibration and validation approach. The adjusted model offers suitable predictions of the gasifier performance under different operating conditions (temperature and equivalence ratio) and for different biomass types. Amongst the gases analysed, H_2 gas was predicted with the lowest accuracy, always being overestimated; the highest absolute error obtained for H_2 was 4.4%. Moreover, the suitability of the model predictions is limited for ER values equal or higher than 0.30.

The tar concentration predicted by the model simulations was between 20 and 42 g/Nm^3 for all biomass types and operating conditions studied; the tar formation was favoured at low ER and temperatures. In addition, for similar ER values, the predicted tar concentration from gasification of eucalyptus was higher than that for pine pellet and pine RFB, which can be related to the biomass particle size, with higher tar concentration associated to the biomass fuel with smaller particles.

Acknowledgments

Authors acknowledge the financial support from the Spanish government (Grant No. FPU15/02653). Thanks are due to FCT/MCTES for the financial support to CESAM (UIDP/50017/2020+UIDB/50017/2020), through national funds.

References

[1] M. Puig-Gamero, J. Argudo-Santamaria, J.L. Valverde, P. Sánchez, L. Sanchez-Silva. Three integrated process simulation using aspen plus®: Pine gasification, syngas cleaning and methanol synthesis. Energy Conversion and Management. 177 (2018) 416-27.

[2] D.T. Pio, L.A.C. Tarelho, M.A.A. Matos. Characteristics of the gas produced during biomass direct gasification in an autothermal pilot-scale bubbling fluidized bed reactor. Energy. 120 (2017) 915-28.

[3] A. Ahmed, A. Salmiaton, T. Choong, W.W. Azlina. Review of kinetic and equilibrium concepts for biomass tar modeling by using Aspen Plus. Renewable and Sustainable Energy Reviews. 52 (2015) 1623-44.

[4] D. Mallick, P. Mahanta, V.S. Moholkar. Co–gasification of coal/biomass blends in 50 kWe circulating fluidized bed gasifier. Journal of the Energy Institute. 93 (2020) 99-111.

[5] H. De Lasa, E. Salaices, J. Mazumder, R. Lucky. Catalytic steam gasification of biomass: catalysts, thermodynamics and kinetics. Chemical Reviews. 111 (2011) 5404-33.

[6] D.T. Pio, L.A.C. Tarelho. Empirical and chemical equilibrium modelling for prediction of biomass gasification products in bubbling fluidized beds. Energy. 202 (2020) 117654.

[7] P. Ji, W. Feng, B. Chen. Production of ultrapure hydrogen from biomass gasification with air. Chemical Engineering Science. 64 (2009) 582-92.

[8] J. Cardoso, V. Silva, D. Eusébio, P. Brito, R.M. Boloy, L. Tarelho, et al. Comparative 2D and 3D analysis on the hydrodynamics behaviour during biomass gasification in a pilot-scale fluidized bed reactor. Renewable Energy. 131 (2019) 713-29.

[9] J. Cardoso, V. Silva, D. Eusébio, P. Brito, M.J. Hall, L. Tarelho. Comparative scaling analysis of two different sized pilot-scale fluidized bed reactors operating with biomass substrates. Energy. 151 (2018) 520-35.

725 [10] P. Ahmed, M.A. Habib, R. Ben-Mansour, P. Kirchen, A.F. Ghoniem. CFD
726 (computational fluid dynamics) analysis of a novel reactor design using ion transport
727 membranes for oxy-fuel combustion. Energy. 77 (2014) 932-44.
728 [11] Y.R. Lee, H.S. Choi, H.C. Park, J.E. Lee. A numerical study on biomass fast pyrolysis
729 process: A comparison between full lumped modeling and hybrid modeling combined with
730 CFD. Computers & Chemical Engineering. 82 (2015) 202-15.
731 [12] R.I. Singh, A. Brink, M. Hupa. CFD modeling to study fluidized bed combustion and
732 gasification. Applied Thermal Engineering. 52 (2013) 585-614.
733 [13] C. Herce, C. Cortés, S. Stendardo. Numerical simulation of a bubbling fluidized bed
734 reactor for sorption-enhanced steam methane reforming under industrially relevant
735 conditions: Effect of sorbent (dolomite and CaO-$Ca_{12}Al_{14}O_{33}$) and operational parameters.
736 Fuel Processing Technology. 186 (2019) 137-48.
737 [14] N.D. Couto, V.B. Silva, E. Monteiro, A. Rouboa. Assessment of municipal solid
738 wastes gasification in a semi-industrial gasifier using syngas quality indices. Energy. 93
739 (2015) 864-73.
740 [15] J.M. de Andrés, M. Vedrenne, M. Brambilla, E. Rodríguez. Modeling and model
741 performance evaluation of sewage sludge gasification in fluidized-bed gasifiers using
742 Aspen Plus. Journal of the Air & Waste Management Association. 69 (2019) 23-33.
743 [16] S. Yang, S. Wang, H. Wang. Numerical study of biomass gasification in a 0.3 MWth
744 full-loop circulating fluidized bed gasifier. Energy Conversion and Management. 223
745 (2020) 113439.
746 [17] L. Vaquerizo, M.J. Cocero. CFD–Aspen Plus interconnection method. Improving
747 thermodynamic modeling in computational fluid dynamic simulations. Computers &
748 Chemical Engineering. 113 (2018) 152-61.

749 [18] S. Beheshti, H. Ghassemi, R. Shahsavan-Markadeh. Process simulation of biomass
750 gasification in a bubbling fluidized bed reactor. Energy Conversion and Management. 94
751 (2015) 345-52.
752 [19] V. Marcantonio, M. De Falco, M. Capocelli, E. Bocci, A. Colantoni, M. Villarini.
753 Process analysis of hydrogen production from biomass gasification in fluidized bed reactor
754 with different separation systems. International Journal of Hydrogen Energy. 44 (2019)
755 10350-60.
756 [20] I.L. Motta, N.T. Miranda, R. Maciel Filho, M.R.W. Maciel. Sugarcane bagasse
757 gasification: Simulation and analysis of different operating parameters, fluidizing media,
758 and gasifier types. Biomass and Bioenergy. 122 (2019) 433-45.
759 [21] P. Kaushal, R. Tyagi. Advanced simulation of biomass gasification in a fluidized bed
760 reactor using ASPEN PLUS. Renewable Energy. 101 (2017) 629-36.
761 [22] D. Pio, L. Tarelho, R. Pinto, M. Matos, J. Frade, A. Yaremchenko, et al. Low-cost
762 catalysts for in-situ improvement of producer gas quality during direct gasification of
763 biomass. Energy. 165 (2018) 442-54.
764 [23] D. Pio, L. Tarelho, A. Tavares, M. Matos, V. Silva. Co-gasification of refused derived
765 fuel and biomass in a pilot-scale bubbling fluidized bed reactor. Energy Conversion and
766 Management. 206 (2020) 112476.
767 [24] J. Haydary. Chemical process design and simulation: Aspen Plus and Aspen Hysys
768 applications. John Wiley & Sons2019.
769 [25] L.P.R. Pala, Q. Wang, G. Kolb, V. Hessel. Steam gasification of biomass with
770 subsequent syngas adjustment using shift reaction for syngas production: An Aspen Plus
771 model. Renewable Energy. 101 (2017) 484-92.

772 [26] D. Neves, H. Thunman, A. Matos, L. Tarelho, A. Gómez-Barea. Characterization and
773 prediction of biomass pyrolysis products. Progress in Energy and Combustion Science. 37
774 (2011) 611-30.
775 [27] A.M. González, E.E.S. Lora, J.C.E. Palacio, O.A.A. del Olmo. Hydrogen production
776 from oil sludge gasification/biomass mixtures and potential use in hydrotreatment
777 processes. International Journal of Hydrogen Energy. 43 (2018) 7808-22.
778 [28] W.M. Champion, C.D. Cooper, K.R. Mackie, P. Cairney. Development of a chemical
779 kinetic model for a biosolids fluidized-bed gasifier and the effects of operating parameters
780 on syngas quality. Journal of the Air & Waste Management Association. 64 (2014) 160-
781 74.
782 [29] Y.C. Choi, X.Y. Li, T.J. Park, J. Kim, J. Lee. Numerical study on the coal gasification
783 characteristics in an entrained flow coal gasifier. Fuel. 80 (2001) 2193-201.
784 [30] G. Groppi, E. Tronconi, P. Forzatti, M. Berg. Mathematical modelling of catalytic
785 combustors fuelled by gasified biomasses. Catalysis Today. 59 (2000) 151-62.
786 [31] L.D. Smoot, P.J. Smith. Coal gasification and combustion. New York: Plenum
787 Press1985.
788 [32] C.K. Westbrook, F.L. Dryer. Chemical kinetic modeling of hydrocarbon combustion.
789 Progress in Energy and Combustion Science. 10 (1984) 1-57.
790 [33] J. Corella, A. Sanz. Modeling circulating fluidized bed biomass gasifiers. A pseudo-
791 rigorous model for stationary state. Fuel Processing Technology. 86 (2005) 1021-53.
792 [34] A. Gómez-Barea, B. Leckner. Modeling of biomass gasification in fluidized bed.
793 Progress in Energy and Combustion Science. 36 (2010) 444-509.
794 [35] K. Umeki, T. Namioka, K. Yoshikawa. Analysis of an updraft biomass gasifier with
795 high temperature steam using a numerical model. Applied Energy. 90 (2012) 38-45.

796 [36] P. Morf, P. Hasler, T. Nussbaumer. Mechanisms and kinetics of homogeneous
797 secondary reactions of tar from continuous pyrolysis of wood chips. Fuel. 81 (2002) 843-
798 53.
799 [37] C.C. Sreejith, C. Muraleedharan, P. Arun. Performance prediction of steam
800 gasification of wood using an ASPEN PLUS thermodynamic equilibrium model.
801 International Journal of Sustainable Energy. 33 (2014) 416-34.
802 [38] Y.D. Kim, C.W. Yang, B.J. Kim, K.S. Kim, J.W. Lee, J.H. Moon, et al. Air-blown
803 gasification of woody biomass in a bubbling fluidized bed gasifier. Applied Energy. 112
804 (2013) 414-20.
805 [39] M.T. Lim, Z. Alimuddin. Bubbling fluidized bed biomass gasification—Performance,
806 process findings and energy analysis. Renewable Energy. 33 (2008) 2339-43.
807 [40] D.A. Bell, B.F. Towler, M. Fan. Coal gasification and its applications. William
808 Andrew2010.
809 [41] J.G. Speight. Heavy oil recovery and upgrading. Gulf Professional Publishing2019.
810 [42] P.-C. Kuo, W. Wu, W.-H. Chen. Gasification performances of raw and torrefied
811 biomass in a downdraft fixed bed gasifier using thermodynamic analysis. Fuel. 117 (2014)
812 1231-41.
813 [43] J.D. Smith, A. Alembath, H. Al-Rubaye, J. Yu, X. Gao, H. Golpour. Validation and
814 application of a kinetic model for downdraft biomass gasification simulation. Chemical
815 Engineering & Technology. 42 (2019) 2505-19.
816 [44] A.Z. Yahaya, M.R. Somalu, A. Muchtar, S.A. Sulaiman, W.R.W. Daud. Effects of
817 temperature on the chemical composition of tars produced from the gasification of coconut
818 and palm kernel shells using downdraft fixed-bed reactor. Fuel. 265 (2020) 116910.

819 [45] N.B. Rasmussen, N. Aryal. Syngas production using straw pellet gasification in
820 fluidized bed allothermal reactor under different temperature conditions. Fuel. 263 (2020)
821 116706.
822 [46] S.M. Atnaw, S.C. Kueh, S.A. Sulaiman. Study on Tar Generated from Downdraft
823 Gasification of Oil Palm Fronds. The Scientific World Journal. 2014 (2014) 497830.
824 [47] T. Mani, P. Murugan, J. Abedi, N. Mahinpey. Pyrolysis of wheat straw in a
825 thermogravimetric analyzer: effect of particle size and heating rate on devolatilization and
826 estimation of global kinetics. Chemical Engineering Research and Design. 88 (2010) 952-
827 8.
828 [48] B.-S. Kang, K.H. Lee, H.J. Park, Y.-K. Park, J.-S. Kim. Fast pyrolysis of radiata pine
829 in a bench scale plant with a fluidized bed: Influence of a char separation system and
830 reaction conditions on the production of bio-oil. Journal of Analytical and Applied
831 Pyrolysis. 76 (2006) 32-7.
832 [49] R. Yin, R. Liu, J. Wu, X. Wu, C. Sun, C. Wu. Influence of particle size on performance
833 of a pilot-scale fixed-bed gasification system. Bioresource Technology. 119 (2012) 15-21.
834 [50] D.T. Pio, L.C.M. Ruivo, L.A.C. Tarelho, J.R. Frade, E. Kantarelis, K. Engvall. Tar
835 formation during eucalyptus gasification in a bubbling fluidized bed reactor: Effect of
836 feedstock and reactor bed composition. Energy Conversion and Management. 229 (2021)
837 113749.

838